CANCER GENOMICS & PROTEOMICS *20*: 88-116 (2023)
doi:10.21873/cgp.20367

SH003 Causes ER Stress-mediated Apoptosis of Breast Cancer Cells *via* Intracellular ROS Production

SEO YEON LEE[1], TAE HOON KIM[1], WON GEUN CHOI[1], YOON HEY CHUNG[2], SEONG-GYU KO[1,2], CHUNHOO CHEON[2] and SUNG-GOOK CHO[3]

[1]*Department of Science in Korean Medicine, Graduate School, Kyung Hee University, Seoul, Republic of Korea;*
[2]*Department of Preventive Medicine, College of Korean Medicine, Kyung Hee University, Seoul, Republic of Korea;*
[3]*Department of Biotechnology, Korea National University of Transportation, Chungbuk, Republic of Korea*

Abstract. *Background/Aim: Breast cancer is one of the most common cancers in women all over the world and new treatment options are urgent. ER stress in cancer cells results in apoptotic cell death, and it is being proposed as a new therapeutic target. SH003, a newly developed herbal medicine, has been reported to have anti-cancer effects. However, its molecular mechanism is not yet clearly defined. Materials and Methods: Microarray was performed to check the differential gene expression patterns in various breast cancer cell lines. Cell viability was measured by MTT assays to detect cytotoxic effects. Annexin V-FITC and 7AAD staining, TUNEL assay and DCF-DA staining were analyzed by flow cytometry to evaluate apoptosis and ROS levels, respectively. Protein expression was examined in SH003-breast cancer cells using immunoblotting assays. The expression of C/EBP Homologous Protein (CHOP) mRNA was measured by real-time PCR. The effects of CHOP by SH003 treatment were investigated using transfection method. Results: Herein, we investigated the molecular mechanisms through which SH003 causes apoptosis of human breast cancer cells. Both cell viability and apoptosis assays confirmed the SH003-induced apoptosis of breast cancer cells. Meanwhile, SH003 altered the expression patterns of several genes in a variety of breast cancer cell lines. More specifically, it upregulated gene sets including the response to unfolded proteins, independently of the breast cancer cell subtype. In addition, SH003-induced apoptosis was due to an increase in ROS production and an activation of the ER stress-signaling pathway. Moreover, CHOP gene silencing blocked SH003-induced apoptosis. Conclusion: SH003 causes apoptosis of breast cancer cells by upregulating ROS production and activating the ER stress-mediated pathway. Thus, our findings suggest that SH003 can be a potential therapeutic agent for breast cancer.*

Correspondence to: Sung-Gook Cho, Department of Biotechnology, Korea National University of Transportation, 61 University Rd., Jeungpyeong, Chungbuk 27909, Republic of Korea. Tel: +82 01062772470, e-mail: chosg@ut.ac.kr; Chunhoo Cheon, Department of Preventive Medicine, College of Korean Medicine, Kyung Hee University, Seoul 02447, Republic of Korea. Tel: +82 01071768535, e-mail: hreedom@khu.ac.kr

Key Words: Breast cancer, SH003, ER stress, ROS, CHOP.

Breast cancer is the second most frequent cancer in women (1). Breast cancer subtypes are classified by expression patterns of three receptor proteins: estrogen receptor (ER), progesterone receptor (PR) and human epidermal growth factor receptor 2 (HER2) (2, 3). Meanwhile, chemotherapeutic agents for breast cancer show side effects and are very expensive (4). Moreover, drug resistance is a hurdle in treating this type of cancer. Herbal medicine is one of the options to solve those problems (5, 6).

SH003 consists of 1:1:1 ratio of *Trichosanthes kirilowii Maxim.*, *Astragalus membranaceu,* and *Angelica gigas* (7). Using network pharmacological approaches, active compounds of SH003 were found to be functionally involved in various pathways that are associated with tumorigenesis and development of cancer. SH003 has been investigated in various cancer cell types to test its anti-cancer effects. In brief, SH003 suppressed tumor growth and metastasis both in cell line experiments *in vitro* and in mouse xenograft studies (7-14). SH003 and classical anti-cancer drugs such as doxorubicin, docetaxel and paclitaxel synergistically inhibited cancer cell growth (9, 14-16). SH003 also repressed tumor angiogenesis by blocking VEGF binding to VEGR2 (17). Thus, SH003 is likely to target various cell types in the tumor microenvironment. Accordingly, we now run clinical studies for SH003 (18-20). More recently, we revealed that

SH003 blocked docetaxel-induced neuropathic pain and ameliorated cyclophosphamide-induced immunosuppression in mouse models (21, 22). Therefore, it is plausible that SH003 plays multifaceted roles in cancer.

Alterations of endoplasmic reticulum (ER) function lead to the accumulation of unfolded or incorrectly folded proteins, a specific condition called ER stress (23). ER stress is involved in the unfolded protein response, an adaptive reaction that maintains the function by reducing the unfolded or misfolded protein load (24). Unfolded protein response (UPR) signaling pathway is mediated by three ER-transmembrane stress sensors: Protein kinase RNA-like ER kinase (PERK), inositol requiring enzyme 1α (IRE1α) and activating transcription factor 6 (ATF6) (25). Especially, the PERK-eIF2α-CHOP pathway results in apoptosis (26, 27). Cancer cells undergo prolonged ER stress, which activates the UPR signaling to restore ER homeostasis (28). Thus, UPR signaling is either cytotoxic or cytoprotective in a cell state-dependent manner (29, 30). However, in cancer cells with excessive ER stress, UPR signaling pathway leads to apoptosis (31). In the process for apoptotic cell death, CHOP is crucial for ER stress-induced apoptosis (26, 32).

We herein investigated the mechanism though which SH003 causes apoptosis of breast cancer cells, independently of the human breast cancer subtype. Our present work shows that SH003 induces apoptotic cell death through intracellular reactive oxygen species (ROS) production and ER stress. Supportively, we revealed that *CHOP* gene silencing rescued SH003-induced apoptosis.

Materials and Methods

Cell culture and transfection. MCF-7, T47D, ZR-75-1, SKBR-3, HCC-1419, MDA-MB-453, HCC-1569, BT-474 and MDA-MB-231 cells were obtained from the American Type Culture Collection (Manassas, VA, USA) and maintained in Dulbecco's Modified Eagle's Medium (Welgene, Seoul, Republic of Korea) supplemented with 10% fetal bovine serum (Gibco, Carlsbad, CA, USA) and 1% penicillin-streptomycin (Welgene). HCC-38 and HCC-70 cells were obtained from the Seoul National University Cell Bank (Seoul, Republic of Korea) and cultured in Roswell Park Memorial Institute Medium-1640 supplemented with 10% fetal bovine serum and 1% penicillin-streptomycin. Breast cancer cell lines were seeded at a density of 2×10^5 cells with antibiotics-free media in 6-well plates. The next day, cells were transfected with 10nmol/mL of either *CHOP* siRNAs or control siRNAs (Bioneer, Daejeon, Republic of Korea) using Lipofectamine RNAiMAX transfection reagent (Invitrogen, Carlsbad, CA, USA) according to the manufacturer's protocol. Medium was replaced with fresh medium including antibiotics at 16 h after transfection, and the cells were treated with SH003 for another 48 h.

Gene expression profiling. RNAs from twelve breast cancer cells (MCF-7, T47D, ZR-75-1, SKBR-3, HCC-1419, MDA-MB-453, HCC-1569, BT-474, MDA-MB-231, HCC-38, HCC70) were isolated using the easy-BLUE RNA Extraction kit (iNtRON Biotech, Sungnam, Republic of Korea), and cDNAs were synthesized and hybridized onto a Human HT12 genome-wide expression profiling chip (Illumina, San Diego, CA, USA). Detection of *p*-Values greater than 0.01 was considered meaningful for analyses, and expression levels greater than 1 were adjusted to 1; both fold changes over 5 and delta difference over 50 with a *t*-test *p*-Value lower than 0.05 were selected. A heat-map was generated for the expression patterns of significant genes. Hierarchical trees were produced by Pearson correlation. Analyses were conducted in Genome Studio software (Illumina), and images were produced in Multiexperimental Viewer (Boston, MA, USA).

Western blot. Cells were lysed in 2× Laemmli sample buffer and boiled at 100˚C for 10 min. Equal quantities of samples were loaded on SDS-PAGE gels (10-15%) and transferred onto nitrocellulose membranes. The membranes were then incubated with primary antibodies. The used primary antibodies were as follows: cleaved Caspase-7 (#9491), cleaved Caspase-8 (#9496), cleaved Caspase-9 (#7237), cleaved PARP (#9541), BIP (ab21685), PERK (#5683), p-PERK (#3197), eIF2α (#9722), p-eIF2α (#3398), IRE1α (#3294), p-IRE1α (PA1-16927), JNK (#3708), p-JNK (#4668), CHOP (#2895) and β-actin (#3700). BIP was obtained from Abcam (Cambridge, UK) and p-IRE1α was purchased from Thermo Fisher Scientific (Waltham, MA, USA). All other antibodies were purchased from Cell Signaling Technology (Danvers, MA, USA).

MTT assay. Cells cultured in 96 well plates were treated with different concentrations of SH003 (0, 50, 100, 250 and 500 μg/ml) for 48 h and then incubated with 5 mg/ml of thiazolyl blue tetrazolium bromide solution for 2 h at 37˚C in the dark. After removing the medium, formazan crystals were solubilized in dimethyl sulfoxide and an absorbance was measured at 575 nm in an ELISA microplate reader.

Annexin V and 7-AAD double staining assay. The rate of apoptotic cells was measured using staining with Annexin V-fluorescein isothiocyanate (FITC) and 7-Aminoactinomycin D (7-AAD). Cells were washed with PBS, trypsinized, re-washed twice with PBS and incubated with FITC-conjugated Annexin-V for 15 min in the dark and 7-AAD for 15 min at room temperature. Next, the samples were measured using BD FACSCalibur flow cytometry. Data were analyzed using Cell Quest software (BD Biosciences, San Jose, CA, USA).

DCF-DA staining assay. Levels of intracellular ROS production were quantified using 2',7'-dichlorofluorescein diacetate (DCF-DA). Cells were plated at 70~80% confluency in 60mm culture dishes. Cells were treated by SH003 at 500 ug/ml for 4 h after N-acetyl-L-cysteine (NAC) treatment for 2 h. The cells were incubated with 10 μM DCF-DA in media for 30 min at 37˚C. Then, the cells were washed with phosphate buffered saline (PBS), trypsinized, resuspended in 0.5 ml of PBS and analyzed by flow cytometry.

TUNEL assay. Apoptotic cells were detected by transferase-mediated deoxyuridine triphosphate (dUTP)-fluorescein nick end-labeling (TUNEL) assay kit (ab66110, Abcam). Forty-eight hours after SH003 treatment, cells were washed with Dulbecco's phosphate buffered saline (DPBS), fixed with 4% paraformaldehyde

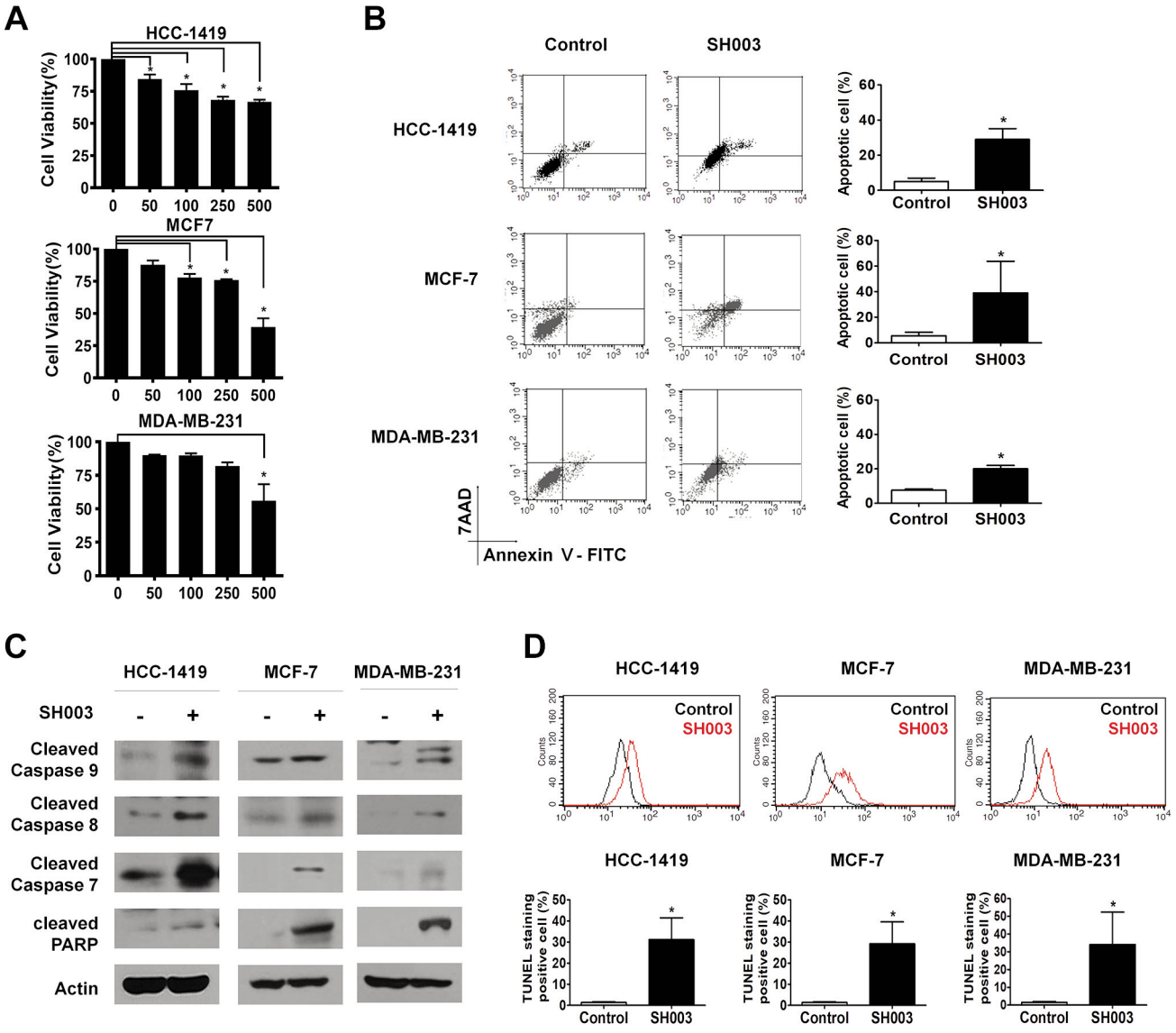

Figure 1. *SH003 induces apoptosis in breast cancer cells. (A) SH003 effect on breast cancer cell viability. HCC-1419, MCF-7 and MBA-MD-231 cells were treated with 0, 50, 100, 250 and 500 μg/ml of SH003 for 48 h. (B) Annexin V-FITC and 7-AAD double-staining assays. Breast cancer cells were treated with SH003 at 500 μg/ml for 48 h. Representative Annexin V-FITC and 7-AAD double-staining data show SH003-induced apoptotic cell death. Bar graphs show apoptotic cell numbers from those analyses. (C) Western blots for cleaved forms of Caspase-9, Caspase-8, Caspase-7, and poly (ADP-ribose) polymerase (PARP). Actin was blotted as the internal loading control. (D) Terminal deoxynucleotidyl transferase dUTP nick end labeling (TUNEL) assays. Representative histograms show SH003-induced apoptotic cell death. Bar graphs show apoptotic cell numbers. All bar graphs are shown as mean and standard deviation of three independent experiments. *p<0.05, Student's t-test.*

for 15 min, washed twice with DPBS and incubated with 70% ethanol. TUNEL reaction was then performed according to the manufacturer's protocol.

RNA isolation and real-time PCR. Cells were seeded in 60mm culture dishes. After SH003 treatment for 48 h, total RNA was isolated using the RNA Easy-blue kit (Qiagen, Germantown, MD, USA) and cDNA was synthesized by reverse transcriptase PCR using the cDNA synthesis kit (Takara, Kusatsu, Shiga, Japan). The SYBR Green PCR Master Mix was used to perform quantitative real-time PCRs. Primers were as follows: *CHOP*-forward: 5-TGG AAA GCA GCG CAT GAA-3, *CHOP*-reverse: 5-AAA GGT GGG TAG TGT GGC -3. *GAPDH*- forward: 5'-TGG ACT CCA CGA CGT ACT CA-3', *GAPDH*-reverse: 5'-AAT CCC ATC ACC ATC TTC CA-3'.

Statistical analysis. All experiments were conducted at least three times. Data were presented as mean and standard deviation, and the analyses were done using Student's *t*-test and one-way analysis of variance (ANOVA) followed by the Bonferroni *post hoc* test. All analyses were done in GraphPad Prism 7 software (San Diego, CA, USA).

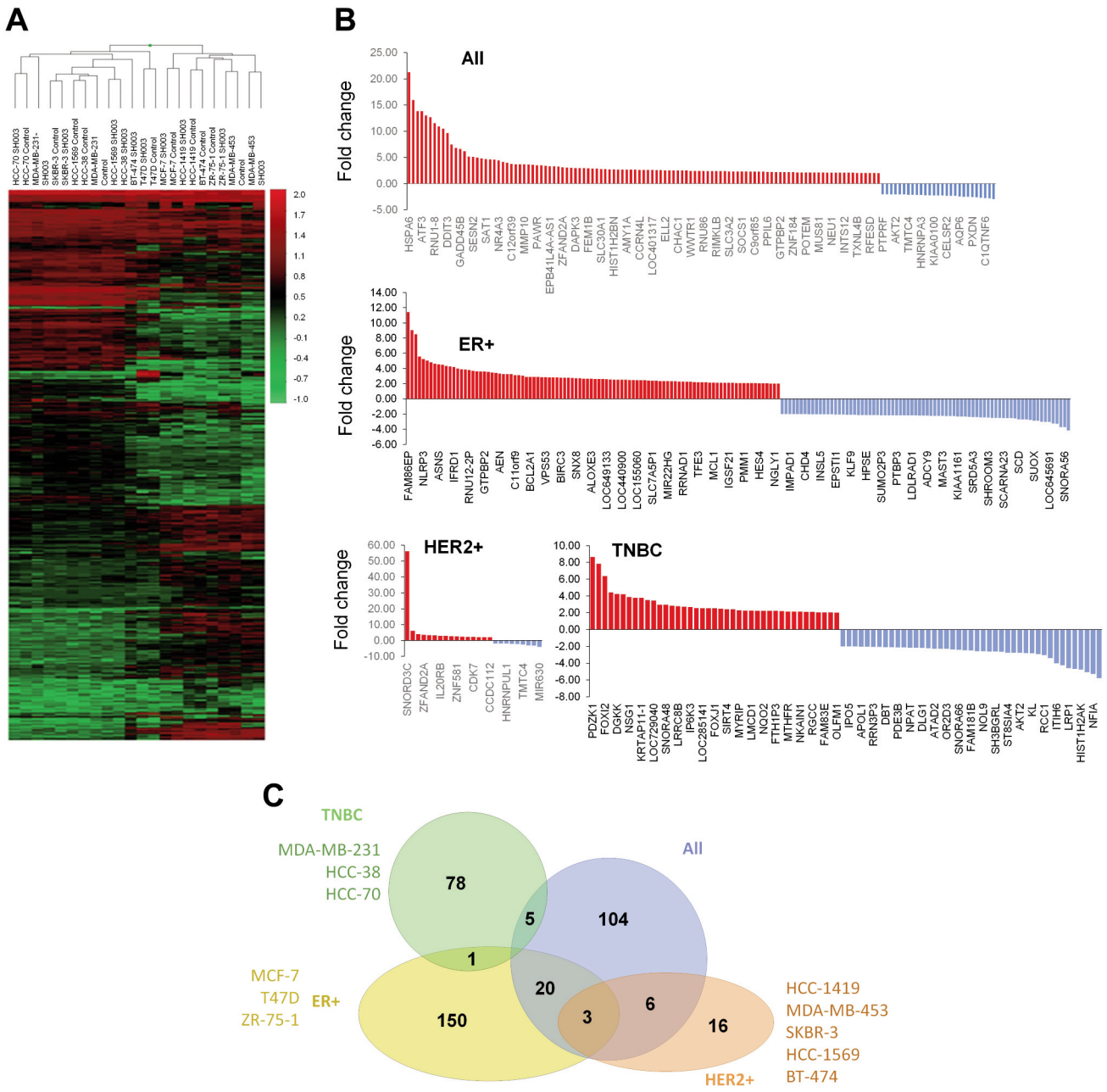

Figure 2. *SH003 alters global gene expression patterns in breast cancer cells. (A) Heatmap produced by hierarchical clustering analysis shows SH003-altered gene expression profiles in various breast cancer cell lines. (B) Genes altered by SH003 in all breast cancer cell lines (All), triple negative breast cancer (TNBC) cell lines, human epidermal growth factor receptor 2 (HER2)+ cell lines, and estrogen receptor (ER)+ cell lines. (C) Venn diagrams representing the number of differentially expressed genes.*

Results

SH003 induces apoptosis in breast cancer cells. To evaluate the cytotoxic effect of SH003 on each subtype of breast cancer cells, we performed MTT assays. The breast cancer cell lines HCC-1419 (HER2-positive), MCF-7 (ER-positive) and MDA-MB-231 (triple-negative) were treated with SH003 (0, 50, 100, 250, 500μg/ml) for 48 h. SH003 decreased the viability of HCC-1419, MCF-7 and MDA-MB-231 cells in a dose-dependent manner (Figure 1A). Accordingly, Annexin V-FITC and 7-AAD double staining assays showed that SH003 causes apoptosis (Figure 1B). SH003 also increased the levels of cleaved Caspase-9, cleaved Caspase-8, cleaved Caspase-7, and cleaved PARP

Table I. *List of differentially expressed genes in all breast cancer cells*.

N	Gene name	Illumina gene name	LLID	Full name	Chr	Exp_ status	Average (CTRL)	Average (SH003)	Fold change	Paired *t*-test	TNOM *p*-Value
1	HSPA6	HSPA6	3310	Heat shock 70kDa protein 6 (HSP70B')	1	Up	26.1	555.8	21.26	0.09	0.0007
2	RNU1-5	RNU1-5	26863	RNA, U1 small nuclear 5	1	Up	99.1	1,579.1	15.94	0.07	0.004
3	SNORD3C	SNORD3C	780853	Small nucleolar RNA, C/D box 3C	17	Up	21.6	299.3	13.85	0.02	0.004
4	ATF3	ATF3	467	Activating transcription factor 3	1	Up	91.8	1268.9	13.82	0.006	0.004
5	SNORD3D	SNORD3D	780854	Small nucleolar RNA, C/D box 3D	17	Up	67.4	877.3	13.01	0.02	0.004
6	HMOX1	HMOX1	3162	Heme oxygenase (decycling) 1	22	Up	130.8	1,659.2	12.68	0.10	0.0007
7	RNU1-8	RNU1F1	26866	RNA, U1 small nuclear 8	14	Up	56.2	648.9	11.54	0.10	0.02
8	SNORD3A	SNORD3A	780851	Small nucleolar RNA, C/D box 3A	17	Up	63.3	691.2	10.92	0.02	0.004
9	FOS	FOS	2353	FBJ murine osteosarcoma viral oncogene homolog	14	Up	56.1	586.7	10.45	0.009	0.0007
10	DDIT3	DDIT3	1649	DNA-damage-inducible transcript 3	12	Up	263.0	2,531.2	9.63	0.008	0.0007
11	HSPA7	HSPA7	3311	Heat shock 70kDa protein 7 (HSP70B)	1	Up	28.2	210.1	7.45	0.14	0.004
12	NR1H4	NR1H4	9971	Nuclear receptor subfamily 1, group H, member 4	12	Up	7.5	50.8	6.81	0.04	0.004
13	GADD45B	GADD45B	4616	Growth arrest and DNA-damage-inducible, beta	19	Up	131.7	874.5	6.64	0.02	0.0007
14	RNU4-2	RNU4-2	26834	RNA, U4 small nuclear 2	12	Up	24.7	152.4	6.18	0.05	0.004
15	ARC	ARC	23237	Activity-regulated cytoskeleton-associated protein	8	Up	26.9	139.0	5.18	0.03	0.004
16	SESN2	SESN2	83667	Sestrin 2	1	Up	43.7	224.1	5.13	0.003	0.004
17	RNU11	RNU11	26824	RNA, U11 small nuclear	1	Up	16.7	82.4	4.94	0.12	0.02
18	NKX2-1	NKX2-1	7080	NK2 homeobox 1	14	Up	2.5	12.1	4.82	0.13	0.004
19	SAT1	SAT1	6303	Spermidine/spermine N1-acetyltransferase 1	X	Up	928.5	4,341.6	4.68	0.007	0.02
20	PPP1R15A	PPP1R15A	23645	Protein phosphatase 1, regulatory subunit 15A	19	Up	784.4	3,623.8	4.62	0.004	0.02
21	DUSP1	DUSP1	1843	Dual specificity phosphatase 1	5	Up	658.3	3,003.7	4.56	0.003	0.004
22	NR4A3	NR4A3	8013	Nuclear receptor subfamily 4, group A, member 3	9	Up	7.4	32.7	4.42	0.10	0.02
23	SRXN1	SRXN1	140809	Sulfiredoxin 1	20	Up	730.6	3,022.8	4.14	0.03	0.004
24	SNHG12	SNHG12	85028	Small nucleolar RNA host gene 12 (non-protein coding)	1	Up	70.0	280.0	4.00	0.01	0.004
25	C12orf39	C12ORF39	80763	Chromosome 12 open reading frame 39	12	Up	4.6	17.1	3.75	0.01	0.004
26	ANGPTL4	ANGPTL4	51129	Angiopoietin-like 4	19	Up	113.5	421.3	3.71	0.15	0.02
27	NFIL3	NFIL3	4783	Nuclear factor, interleukin 3 regulated	9	Up	99.9	368.9	3.69	0.007	0.0007
28	MMP10	MMP10	4319	Matrix metallopeptidase 10 (stromelysin 2)	11	Up	8.1	29.8	3.67	0.01	0.004
29	DUSP5	DUSP5	1847	Dual specificity phosphatase 5	10	Up	810.0	2,966.7	3.66	0.002	0.0007
30	UBE2HP1	LOC646463	646463	Ubiquitin-conjugating enzyme E2H pseudogene 1	8	Up	103.0	369.3	3.59	0.006	0.004

Table I. *Continued*

Table I. *Continued*

N	Gene name	Illumina gene name	LLID	Full name	Chr	Exp_ status	Average (CTRL)	Average (SH003)	Fold change	Paired *t*-test	TNOM *p*-Value
31	PAWR	PAWR	5074	PRKC, apoptosis, WT1, regulator	12	Up	177.8	625.0	3.51	0.01	0.004
32	C2CD4B	C2CD4B	388125	C2 calcium-dependent domain containing 4B	15	Up	5.1	17.8	3.50	0.01	0.004
33	BEX2	BEX2	84707	Brain expressed X-linked 2	X	Up	142.1	484.9	3.41	0.004	0.02
34	EPB41L4A-AS1	TIGA1	114915	EPB41L4A antisense RNA 1	5	Up	559.8	1,844.9	3.30	0.003	0.02
35	TAF1D	TAF1D	79101	TATA box binding protein (TBP)-associated factor, RNA polymerase I, D, 41kDa	11	Up	28.8	94.6	3.28	0.006	0.004
36	RNU12-2P	RNU12	26823	RNA, U12 small nuclear 2, pseudogene	X	Up	7.8	25.1	3.23	0.007	0.02
37	ZFAND2A	ZFAND2A	90637	Zinc finger, AN1-type domain 2A	7	Up	424.1	1,321.6	3.12	0.003	0.0007
38	ZNF460	ZNF460	10794	Zinc finger protein 460	19	Up	10.5	32.2	3.06	0.09	0.02
39	DNAJB9	DNAJB9	4189	DnaJ (Hsp40) homolog, subfamily B, member 9	7	Up	166.3	503.4	3.03	0.02	0.02
40	DAPK3	DAPK3	1613	Death-associated protein kinase 3	19	Up	72.0	213.7	2.97	0.02	0.02
41	GPCPD1	RP5-1022P6.2	56261	Glycerophosphocholine phosphodiesterase GDE1 homolog (S. cerevisiae)	20	Up	44.1	130.4	2.96	0.08	0.004
42	LOC285141	LOC285141	285141	Uncharacterized protein LOC285141	2	Up	16.0	46.9	2.94	0.008	0.004
43	FEM1B	FEM1B	10116	Fem-1 homolog b (C. elegans)	15	Up	34.9	101.3	2.90	0.09	0.02
44	ACTG1P4	LOC648740	648740	Actin, gamma 1 pseudogene 4	1	Up	99.0	285.7	2.89	0.02	0.02
45	SERTAD1	SERTAD1	29950	SERTA domain containing 1	19	Up	486.0	1,401.1	2.88	0.007	0.02
46	SLC30A1	SLC30A1	7779	Solute carrier family 30 (zinc transporter), member 1	1	Up	118.5	327.3	2.76	0.001	0.0007
47	RGCC	C13ORF15	28984	Regulator of cell cycle	13	Up	44.4	121.9	2.74	0.02	0.02
48	CCNB1IP1	CCNB1IP1	57820	Cyclin B1 interacting protein 1, E3 ubiquitin protein ligase	14	Up	162.4	439.7	2.71	0.002	0.02
49	HIST1H2BN	HIST1H2BN	8341	Histone cluster 1, H2bn	6	Up	14.7	39.6	2.70	0.04	0.02
50	SNHG15	C7ORF40	285958	Small nucleolar RNA host gene 15 (non-protein coding)	7	Up	340.6	916.7	2.69	0.003	0.004
51	C3orf78	SNHG8	440957	Chromosome 3 open reading frame 78	3	Up	155.7	417.4	2.68	0.03	0.004
52	AMY1A	AMY1A	276	Amylase, alpha 1A (salivary)	1	Up	130.0	345.3	2.66	0.01	0.02
53	MIR507	MIR507	574512	MicroRNA 507	X	Up	12.3	32.7	2.65	0.0005	6.2×10^{-5}
54	C6orf48	C6ORF48	50854	Chromosome 6 open reading frame 48	6	Up	669.1	1,772.6	2.65	0.006	0.004
55	CCRN4L	CCRN4L	25819	CCR4 carbon catabolite repression 4-like (S. cerevisiae)	4	Up	75.7	200.1	2.64	0.04	0.02
56	ADPRM	C17ORF48	56985	ADP-ribose/CDP-alcohol diphosphatase, manganese-dependent	17	Up	75.8	199.1	2.63	0.006	0.02
57	PHF2P1	DKFZP686A1627	266695	PHD finger protein 2 pseudogene 1	13	Up	4.3	11.1	2.61	0.05	0.004
58	LOC401317	LOC401317	401317	Uncharacterized LOC401317	7	Up	23.9	62.0	2.60	0.008	0.02
59	C2orf49	C2ORF49	79074	Chromosome 2 open reading frame 49	2	Up	125.0	321.7	2.57	0.004	0.004
60	C20orf111	C20ORF111	51526	Chromosome 20 open reading frame 111	20	Up	948.6	2,423.9	2.56	0.007	0.004
61	ELL2	ELL2	22936	Elongation factor, RNA polymerase II, 2	5	Up	86.8	220.9	2.54	0.004	0.02
62	LOC285299	LOC285299	285299	FSHD region gene 2 family, member C-like	3	Up	5.1	13.0	2.53	0.04	0.004

Table I. *Continued*

Table I. *Continued*

N	Gene name	Illumina gene name	LLID	Full name	Chr	Exp_ status	Average (CTRL)	Average (SH003)	Fold change	Paired *t*-test	TNOM *p*-Value
63	RNF19B	RNF19B	127544	Ring finger protein 19B	1	Up	103.4	261.1	2.53	0.007	0.0007
64	CHAC1	CHAC1	79094	ChaC, cation transport regulator homolog 1 (E. coli)	15	Up	38.1	96.1	2.52	0.0008	0.02
65	HSPBAP1	HSPBAP1	79663	HSPB (heat shock 27kDa) associated protein 1	3	Up	50.4	126.4	2.51	0.007	0.0007
66	KDM3A	JMJD1A	55818	Lysine (K)-specific demethylase 3A	2	Up	75.7	189.2	2.50	0.02	0.004
67	WWTR1	WWTR1	25937	WW domain containing transcription regulator 1	3	Up	17.5	42.6	2.44	0.02	0.004
68	SAMD8	SAMD8	142891	Sterile alpha motif domain containing 8	10	Up	15.0	36.4	2.42	0.002	0.004
69	BLOC1S2	BLOC1S2	282991	Biogenesis of lysosomal organelles complex-1, subunit 2	10	Up	43.5	104.9	2.41	0.005	0.02
70	RNU86	RNU86	116936	RNA, U86 small nucleolar	22	Up	42.5	101.9	2.40	0.002	0.004
71	GCLM	GCLM	2730	Glutamate-cysteine ligase, modifier subunit	1	Up	380.2	907.7	2.39	0.001	0.02
72	IL20RB	IL20RB	53833	Interleukin 20 receptor beta	3	Up	21.4	50.8	2.38	0.06	0.02
73	RIMKLB	FAM80B	57494	Ribosomal modification protein rimK-like family member B	12	Up	25.1	59.3	2.36	0.006	0.02
74	RNU4ATAC	RNU4ATAC	100151683	RNA, U4atac small nuclear (U12-dependent splicing)	2	Up	25.6	60.5	2.36	0.03	0.004
75	GABPB1	GABPB1	2553	GA binding protein transcription factor, beta subunit 1	15	Up	46.3	109.2	2.36	0.11	0.02
76	SLC3A2	SLC3A2	6520	Solute carrier family 3 (activators of dibasic and neutral amino acid transport), member 2	11	Up	718.9	1,679.9	2.34	0.001	0.02
77	IFRD1	IFRD1	3475	Interferon-related developmental regulator 1	7	Up	135.7	316.1	2.33	0.01	0.02
78	ZYX	ZYX	7791	Zyxin	7	Up	494.4	1140.6	2.31	0.02	0.02
79	SOCS1	SOCS1	8651	Suppressor of cytokine signaling 1	16	Up	40.3	93.0	2.31	0.04	0.02
80	ZMYM5	ZMYM5	9205	Zinc finger, MYM-type 5	13	Up	43.4	100.1	2.30	0.02	0.004
81	RND3	RND3	390	Rho family GTPase 3	2	Up	319.4	734.4	2.30	0.01	0.004
82	C9orf85	C9ORF85	138241	Chromosome 9 open reading frame 85	9	Up	39.3	89.5	2.27	0.005	0.004
83	STX1A	STX1A	6804	Syntaxin 1A (brain)	7	Up	147.5	335.0	2.27	0.007	0.004
84	RP9P	RP9P	441212	Retinitis pigmentosa 9 pseudogene	7	Up	36.0	81.8	2.27	0.001	0.02
85	PPIL6	PPIL6	285755	Peptidylprolyl isomerase (cyclophilin)-like 6	6	Up	10.7	23.8	2.22	0.01	0.02
86	EID3	EID3	493861	EP300 interacting inhibitor of differentiation 3	12	Up	13.5	29.7	2.21	0.0009	0.004
87	SLMO1	SLMO1	10650	Slowmo homolog 1 (Drosophila)	18	Up	60.1	132.4	2.20	0.002	0.02
88	GTPBP2	GTPBP2	54676	GTP binding protein 2	6	Up	41.4	91.1	2.20	0.006	0.004
89	CIDECP	CIDECP	152302	Cell death-inducing DFFA-like effector c pseudogene	3	Up	38.1	83.7	2.20	0.001	0.004
90	LOC143666	LOC143666	143666	Uncharacterized LOC143666	11	Up	112.5	245.0	2.18	0.0004	0.02
91	ZNF184	ZNF184	7738	Zinc finger protein 184	6	Up	31.6	68.2	2.16	0.03	0.02
92	C3orf71	C3ORF71	646450	Chromosome 3 open reading frame 71	3	Up	17.2	37.0	2.15	0.0002	0.0007
93	SNORD10	SNORD10	652966	Small nucleolar RNA, C/D box 10	17	Up	10.7	23.0	2.15	0.01	0.02

Table I. *Continued*

Table I. *Continued*

N	Gene name	Illumina gene name	LLID	Full name	Chr	Exp_ status	Average (CTRL)	Average (SH003)	Fold change	Paired *t*-test	TNOM *p*-Value
94	POTEM	P704P	641455	POTE ankyrin domain family, member M	14	Up	116.3	248.7	2.14	0.04	0.02
95	HIST1H1C	HIST1H1C	3006	Histone cluster 1, H1c	6	Up	589.2	1246.3	2.12	0.007	0.004
96	CCDC130	CCDC130	81576	Coiled-coil domain containing 130	19	Up	336.1	710.2	2.11	0.008	0.02
97	MUS81	MUS81	80198	MUS81 endonuclease homolog (S. cerevisiae)	11	Up	244.6	515.9	2.11	0.004	0.0007
98	CEBPG	CEBPG	1054	CCAAT/enhancer binding protein (C/EBP), gamma	19	Up	378.1	797.0	2.11	0.006	0.02
99	PITHD1	C1ORF128	57095	PITH (C-terminal proteasome-interacting domain of thioredoxin-like) domain containing 1	1	Up	603.6	1,269.4	2.10	0.003	0.004
100	NEU1	NEU1	4758	Sialidase 1 (lysosomal sialidase)	6	Up	466.7	979.1	2.10	0.002	0.02
101	SNHG5	SNHG5	387066	Small nucleolar RNA host gene 5 (non-protein coding)	6	Up	2,790.5	5,830.6	2.09	0.002	0.02
102	C1orf162	C1ORF162	128346	Chromosome 1 open reading frame 162	1	Up	24.5	51.2	2.09	0.04	0.004
103	INTS12	INTS12	57117	Integrator complex subunit 12	4	Up	369.1	770.4	2.09	0.001	0.0007
104	FOSB	FOSB	2354	FBJ murine osteosarcoma viral oncogene homolog B	19	Up	68.9	143.1	2.08	0.08	0.004
105	LOC284023	LOC284023	284023	Uncharacterized LOC284023	17	Up	61.5	126.9	2.06	0.02	0.004
106	TXNL4B	TXNL4B	54957	Thioredoxin-like 4B	16	Up	30.5	62.5	2.05	0.0009	0.0007
107	THAP10	THAP10	56906	THAP domain containing 10	15	Up	67.7	138.5	2.05	0.01	0.02
108	HABP4	HABP4	22927	Hyaluronan binding protein 4	9	Up	79.4	161.9	2.04	0.0009	0.004
109	RFESD	RFESD	317671	Rieske (Fe-S) domain containing	5	Up	68.9	140.0	2.03	0.001	0.02
110	POLR3C	POLR3C	10623	Polymerase (RNA) III (DNA directed) polypeptide C (62kD)	1	Up	439.3	883.0	2.01	0.007	0.02
111	C9orf9	C9ORF9	11092	Chromosome 9 open reading frame 9	9	Up	31.8	63.9	2.01	0.02	0.02
112	PTPRF	PTPRF	5792	Protein tyrosine phosphatase, receptor type, F	1	Down	917.7	453.0	–2.03	0.01	0.004
113	XXYLT1	C3ORF21	152002	Xyloside xylosyltransferase 1	3	Down	287.8	142.0	–2.03	0.005	0.02
114	SH3BGRL	SH3BGRL	6451	SH3 domain binding glutamic acid-rich protein like	X	Down	127.4	62.1	–2.05	0.003	0.004
115	AKT2	AKT2	208	V-akt murine thymoma viral oncogene homolog 2	19	Down	13.8	6.7	–2.07	0.03	0.004
116	STS	STS	412	Steroid sulfatase (microsomal), isozyme S	X	Down	19.5	9.4	–2.08	0.01	0.02
117	HNRNPUL1	HNRPUL1	11100	Heterogeneous nuclear ribonucleoprotein U-like 1	19	Down	1,019.1	488.3	–2.09	0.0007	0.004
118	TMTC4	TMTC4	84899	Transmembrane and tetratricopeptide repeat containing 4	13	Down	46.4	22.1	–2.10	0.05	0.0007
119	CTGLF8P	LOC728608	728608	Centaurin, gamma-like family, member 8 pseudogene	10	Down	14.9	7.0	–2.12	0.005	0.02
120	AP2B1	AP2B1	163	Adaptor-related protein complex 2, beta 1 subunit	17	Down	134.5	62.9	–2.14	0.004	0.004
121	HNRNPA3	HNRNPA3	220988	Heterogeneous nuclear ribonucleoprotein A3	2	Down	392.3	179.7	–2.18	0.008	0.004
122	GALNT10	GALNT10	55568	UDP-N-acetyl-alpha-D-galactosamine:polypeptide N-acetylgalactosaminyltransferase 10 (GalNAc-T10)	5	Down	85.1	38.8	–2.19	0.01	0.02

Table I. *Continued*

Table I. *Continued*

N	Gene name	Illumina gene name	LLID	Full name	Chr	Exp_ status	Average (CTRL)	Average (SH003)	Fold change	Paired *t*-test	TNOM *p*-Value
123	ZADH2	ZADH2	284273	Zinc binding alcohol dehydrogenase domain containing 2	18	Down	117.4	52.6	–2.23	0.05	0.02
124	KIAA0100	KIAA0100	9703	KIAA0100	17	Down	130.5	58.2	–2.24	0.003	0.02
125	REEP5	REEP5	7905	Receptor accessory protein 5	5	Down	916.4	406.1	–2.26	0.003	0.02
126	PIK3R2	PIK3R2	5296	Phosphoinositide-3-kinase, regulatory subunit 2 (beta)	19	Down	1,654.3	729.6	–2.27	0.004	0.02
127	CELSR2	CELSR2	1952	Cadherin, EGF LAG seven-pass G-type receptor 2 (flamingo homolog, Drosophila)	1	Down	105.2	45.3	–2.32	0.006	0.02
128	PIGU	PIGU	128869	Phosphatidylinositol glycan anchor biosynthesis, class U	20	Down	455.0	196.0	–2.32	0.06	0.004
129	MIR181B1	MIR181B1	406955	MicroRNA 181b-1	1	Down	6.5	2.8	–2.33	0.02	0.02
130	AQP6	AQP6	363	Aquaporin 6, kidney specific	12	Down	16.4	6.7	–2.45	0.03	0.02
131	GREM2	GREM2	64388	Gremlin 2	1	Down	9.6	3.9	–2.49	0.02	0.02
132	RRM2	RRM2	6241	Ribonucleotide reductase M2	2	Down	245.1	98.1	–2.50	0.02	0.02
133	PXDN	PXDN	7837	Peroxidasin homolog (Drosophila)	2	Down	344.0	133.7	–2.57	0.02	0.02
134	FZD4	FZD4	8322	Frizzled family receptor 4	11	Down	125.5	48.3	–2.60	0.006	0.02
135	BCL2	BCL2	596	B-cell CLL/lymphoma 2	18	Down	65.8	24.2	–2.72	0.06	0.02
136	C1QTNF6	C1QTNF6	114904	C1q and tumor necrosis factor related protein 6	22	Down	55.6	20.1	–2.76	0.04	0.02
137	TNS3	TNS3	64759	Tensin 3	7	Down	378.2	135.3	–2.80	0.007	0.004
138	MCCC2	MCCC2	64087	Methylcrotonoyl-CoA carboxylase 2 (beta)	5	Down	78.0	26.4	–2.95	0.002	0.02

Cut-off: fold change>2, *p*-Value <0.5. LLID: Locus link ID; TNoM: threshold number of misclassification.

(Figure 1C). Consistently, SH003 increased apoptotic cell number in TUNEL assays (Figure 1D). Thus, our data indicate that SH003 induces apoptosis independently of the breast cancer cells line.

SH003 alters expression patterns of gene in breast cancer cells. To investigate the genes affected by SH003 in breast cancer cells, we analyzed differential gene expression patterns between non-treated and SH003-treated breast cancer cells. Various breast cancer cell lines representing different breast cancer subtypes were used in the experiment as follows: ER-positive (MCF-7, T47D and ZR-75-1), HER2-positive (SKBR-3, HCC-1419, MDA-MB-453, HCC-1569 and BT-474) and triple-negative (MDA-MB-231, HCC-38 and HCC70). A heatmap for the expression levels of 31,823 genes is shown in Figure 2A. SH003 upregulated 111 genes and downregulated 27 genes independently of subtypes (cut-off over 2-fold change, *p*-Value <0.5) (Figure 2B, C, and Table I). SH003 subtype-specifically affected 84 genes in triple-negative breast cancer cells, 25 genes in HER2-positive breast cancer cells and 174 genes in ER-positive breast cancer cells (Figure 2B and C, Table II, Table III, and Table IV). Next, we conducted gene ontology analysis for gene set enrichment. SH003 upregulated gene sets including 'response to unfolded protein' in biological process, 'transcription corepressor activity' in molecular function and 'nucleus' in cellular component, and downregulated 'receptor tyrosine kinase binding' in molecular function (Table V). While SH003 altered gene sets in ER-positive breast cancer cells, it did not alter gene sets in triple-negative and HER2-positive breast cancer cells. KEGG analysis for biological pathway showed that SH003 altered 20 pathways including the phosphatidylinositol signaling system, MAPK signaling pathway and apoptosis (Table VI).

SH003 causes apoptosis by activating ER stress. Among 138 genes, SH003 strongly altered the expression levels of *SNORD3C*, *ATF3*, *SNORD3D*, *SNORD3A*, *FOS*, *DDIT3* (also called *GADD153* or *CHOP*), *NR1H4* (*FXR* or *RIP14*), *GADD45B (MyD118)*, *ARC* (*ARG3.1*) and *SESN2* in terms of fold-change >5, *p*-Value <0.05 by paired *t*-test and Total Number of Misclassifications (TNoM) (Table I). Considering the top 10 genes upregulated by SH003 (Table I) and data from gene ontology and KEGG (Table V and Table VI), we hypothesized that SH003 might cause apoptotic cell death by activating ER

Table II. *List of differentially expressed genes in triple-negative breast cancer cells*.

N	Gene name	Illumina gene name	LLID	Full name	Chr	Exp_ status	Average (TNBC control)	Average (TNBC SH003)	Fold change	Paired *t*-test
1	PDZK1	PDZK1	5174	PDZ domain containing 1	1	Up	1.7	14.5	8.66	0.03
2	ZC3H6	ZC3H6	376940	Zinc finger CCCH-type containing 6	2	Up	2.2	17.0	7.83	0.01
3	FOXI2	FOXI2	399823	Forkhead box I2	10	Up	2.2	14.0	6.38	0.04
4	CDH17	CDH17	1015	Cadherin 17, LI cadherin (liver-intestine)	8	Up	2.0	8.8	4.42	0.02
5	DGKK	DGKK	139189	Diacylglycerol kinase, kappa	X	Up	2.2	9.1	4.24	0.05
6	FMN2	FMN2	56776	Formin 2	1	Up	2.3	9.8	4.21	0.01
7	NSG1	D4S234E	27065	Neuron specific gene family member 1	4	Up	2.0	7.7	3.86	0.05
8	SMAD9	SMAD9	4093	SMAD family member 9	13	Up	3.0	11.4	3.78	0.008
9	KRTAP11-1	KRTAP11-1	337880	Keratin associated protein 11-1	21	Up	5.2	19.6	3.77	0.003
10	LOC441461	LOC441461	441461	Uncharacterized LOC441461	9	Up	4.9	17.4	3.51	0.03
11	LOC729040	LOC729040	729040	Uncharacterized LOC729040	5	Up	5.3	18.3	3.46	0.05
12	BPIFA2	C20ORF70	140683	BPI fold containing family A, member 2	20	Up	7.6	22.5	2.95	0.01
13	SNORA48	SNORA48	652965	Small nucleolar RNA, H/ACA box 48	17	Up	4.5	13.2	2.95	0.008
14	LOC100132116	LOC100132116	100132116	Uncharacterized LOC100132116	10	Up	5.1	14.4	2.83	0.02
15	LRRC8B	LRRC8B	23507	Leucine rich repeat containing 8 family, member B	1	Up	5.4	14.8	2.76	0.03
16	STX19	STX19	415117	Syntaxin 19	3	Up	5.1	13.7	2.70	0.02
17	IP6K3	IHPK3	117283	Inositol hexakisphosphate kinase 3	6	Up	7.8	20.9	2.67	0.0007
18	LEAP2	LEAP2	116842	Liver expressed antimicrobial peptide 2	5	Up	8.8	22.6	2.57	0.03
19	LOC285141	LOC285141	285141	Uncharacterized protein LOC285141	2	Up	23.6	60.1	2.54	0.03
20	SLC6A17	SLC6A17	388662	Solute carrier family 6, member 17	1	Up	7.1	18.1	2.54	0.02
21	FOXJ1	FOXJ1	2302	Forkhead box J1	17	Up	4.2	10.6	2.52	0.006
22	KCNMB4	KCNMB4	27345	Potassium large conductance calcium-activated channel, subfamily M, beta member 4	12	Up	11.1	27.3	2.46	0.01
23	SIRT4	SIRT4	23409	Sirtuin 4	12	Up	19.4	46.8	2.42	0.02
24	TFAP2B	TFAP2B	7021	Transcription factor AP-2 beta (activating enhancer binding protein 2 beta)	6	Up	2.2	5.2	2.41	0.02
25	MYRIP	MYRIP	25924	Myosin VIIA and Rab interacting protein	3	Up	6.7	15.2	2.28	0.05
26	GNG4	GNG4	2786	Guanine nucleotide binding protein (G protein), gamma 4	1	Up	5.9	13.5	2.27	0.03
27	LMCD1	LMCD1	29995	LIM and cysteine-rich domains 1	3	Up	43.0	96.9	2.25	0.03
28	HOMER2	HOMER2	9455	Homer homolog 2 (Drosophila)	15	Up	92.1	205.0	2.23	0.03
29	NQO2	NQO2	4835	NAD(P)H dehydrogenase, quinone 2	6	Up	305.3	677.6	2.22	0.03
30	PTPRD	PTPRD	5789	Protein tyrosine phosphatase, receptor type, D	9	Up	4.1	9.1	2.22	0.02
31	FTH1P3	FTHL3	2498	Ferritin, heavy polypeptide 1 pseudogene 3	2	Up	378.0	837.0	2.21	0.05
32	FLJ37786	FLJ37786	642691	Uncharacterized LOC642691	2	Up	9.4	20.6	2.19	0.03
33	MTHFR	MTHFR	4524	Methylenetetrahydrofolate reductase [NAD(P)H]	1	Up	18.7	40.3	2.15	0.004
34	GOLGA8A	GOLGA8A	23015	Golgin A8 family, member A	15	Up	7.8	16.6	2.14	0.04
35	NKAIN1	NKAIN1	79570	Na+/K+ transporting ATPase interacting 1	1	Up	4.3	9.2	2.12	0.003
36	FTH1P2	FTHL2	2497	Ferritin, heavy polypeptide 1 pseudogene 2	1	Up	112.5	238.0	2.12	0.01
37	RGCC	C13ORF15	28984	Regulator of cell cycle	13	Up	71.3	149.0	2.09	0.003
38	PFKFB1	PFKFB1	5207	6-phosphofructo-2-kinase/ fructose-2,6-biphosphatase 1	X	Up	7.7	15.7	2.05	0.01
39	FAM83E	FAM83E	54854	Family with sequence similarity 83, member E	19	Up	4.0	8.2	2.05	0.03
40	MKRN3	MKRN3	7681	Makorin ring finger protein 3	15	Up	9.2	18.9	2.04	0.04
41	OLFM1	OLFM1	10439	Olfactomedin 1	9	Up	4.1	8.2	2.00	0.002
42	RAET1K	RAET1K	646024	Retinoic acid early transcript 1K pseudogene	6	Down	22.8	11.4	–2.00	0.05
43	IPO5	IPO5	3843	Importin 5	13	Down	192.2	95.6	–2.01	0.05
44	C1QTNF6	C1QTNF6	114904	C1q and tumor necrosis factor related protein 6	22	Down	29.1	14.4	–2.02	0.04
45	APOL1	APOL1	8542	Apolipoprotein L, 1	22	Down	5.1	2.5	–2.04	0.02

Table II. *Continued*

Table II. *Continued*

N	Gene name	Illumina gene name	LLID	Full name	Chr	Exp_ status	Average (TNBC control)	Average (TNBC SH003)	Fold change	Paired *t*-test
46	SMCR5	SMCR5	140771	Smith-Magenis syndrome chromosome region, candidate 5 (non-protein coding)	17	Down	44.1	21.5	–2.05	0.04
47	RRN3P3	LOC100131998	100131998	RNA polymerase I transcription factor homolog (S. cerevisiae) pseudogene 3	16	Down	30.8	14.9	–2.06	0.01
48	TAS2R8	TAS2R8	50836	Taste receptor, type 2, member 8	12	Down	6.3	3.0	–2.06	0.03
49	DBT	DBT	1629	Dihydrolipoamide branched chain transacylase E2	1	Down	26.8	12.9	–2.09	0.04
50	GGT7	GGT7	2686	Gamma-glutamyltransferase 7	20	Down	17.7	8.4	–2.10	0.04
51	PDE3B	PDE3B	5140	Phosphodiesterase 3B, cGMP-inhibited	11	Down	25.8	12.2	–2.11	0.04
52	PPP1R9A	PPP1R9A	55607	Protein phosphatase 1, regulatory subunit 9A	7	Down	9.6	4.5	–2.12	0.04
53	NPAT	NPAT	4863	Nuclear protein, ataxia-telangiectasia locus	11	Down	67.0	31.0	–2.16	0.03
54	SMARCA2	SMARCA2	6595	SWI/SNF related, matrix associated, actin dependent regulator of chromatin, subfamily a, member 2	9	Down	197.4	91.1	–2.17	0.03
55	DLG1	DLG1	1739	Discs, large homolog 1 (Drosophila)	3	Down	36.5	16.6	–2.19	0.01
56	AGR2	AGR2	10551	Anterior gradient 2 homolog (Xenopus laevis)	7	Down	12.3	5.5	–2.22	0.05
57	ATAD2	ATAD2	29028	ATPase family, AAA domain containing 2	8	Down	420.5	185.4	–2.27	0.03
58	MORC2-AS1	FLJ35801	150291	MORC2 antisense RNA 1	22	Down	18.8	8.2	–2.28	0.03
59	OR2D3	OR2D3	120775	Olfactory receptor, family 2, subfamily D, member 3	11	Down	19.3	8.4	–2.29	0.03
60	MYO7B	MYO7B	4648	Myosin VIIB	2	Down	7.3	3.0	–2.38	0.03
61	SNORA66	SNORA66	26782	Small nucleolar RNA, H/ACA box 66	1	Down	23.8	9.9	–2.41	0.004
62	EXOC5P1	LOC644548	644548	Exocyst complex component 5 pseudogene 1	4	Down	9.2	3.7	–2.46	0.001
63	FAM181B	FAM181B	220382	Family with sequence similarity 181, member B	11	Down	9.3	3.7	–2.50	0.02
64	SIGLEC12	SIGLEC12	89858	Sialic acid binding Ig-like lectin 12 (gene/pseudogene)	19	Down	11.0	4.3	–2.57	0.02
65	NOL9	NOL9	79707	Nucleolar protein 9	1	Down	21.3	8.2	–2.58	0.02
66	LOC400768	LOC400768	400768	Uncharacterized LOC400768	1	Down	13.8	5.3	–2.62	0.02
67	SH3BGRL	SH3BGRL	6451	SH3 domain binding glutamic acid-rich protein like	X	Down	103.1	39.2	–2.63	0.03
68	FGF19	FGF19	9965	Fibroblast growth factor 19	11	Down	12.0	4.6	–2.64	0.006
69	ST8SIA4	ST8SIA4	7903	ST8 alpha-N-acetyl-neuraminide alpha-2,8-sialyltransferase 4	5	Down	11.5	4.2	–2.75	0.03
70	SPTLC3	SPTLC3	55304	Serine palmitoyltransferase, long chain base subunit 3	20	Down	18.2	6.6	–2.76	0.008
71	AKT2	AKT2	208	V-Akt murine thymoma viral oncogene homolog 2	19	Down	9.6	3.5	–2.77	0.03
72	XRCC5	XRCC5	7520	X-ray repair complementing defective repair in Chinese hamster cells 5 (double-strand-break rejoining)	2	Down	466.3	167.1	–2.79	0.03
73	KL	KL	9365	Klotho	13	Down	9.7	3.4	–2.84	0.05
74	SNORD51	SNORD51	26798	Small nucleolar RNA, C/D box 51	2	Down	18.0	6.2	–2.92	0.004
75	RCC1	RCC1	1104	Regulator of chromosome condensation 1	1	Down	29.6	9.8	–3.03	0.007
76	SLC52A1	GPR172B	55065	Solute carrier family 52, riboflavin transporter, member 1	17	Down	14.8	4.3	–3.42	0.002

Table II. *Continued*

Table II. *Continued*

N	Gene name	Illumina gene name	LLID	Full name	Chr	Exp_ status	Average (TNBC control)	Average (TNBC SH003)	Fold change	Paired *t*-test
77	ITIH6	ITIH5L	347365	Inter-alpha-trypsin inhibitor heavy chain family, member 6	X	Down	9.5	2.4	–4.02	0.006
78	C11orf52	C11ORF52	91894	Chromosome 11 open reading frame 52	11	Down	14.4	3.4	–4.27	0.009
79	LRP1	LRP1	4035	Low density lipoprotein receptor-related protein 1	12	Down	10.5	2.3	–4.60	0.002
80	SOWAHA	ANKRD43	134548	Sosondowah ankyrin repeat domain family member A	5	Down	8.6	1.8	–4.67	0.003
81	HIST1H2AK	HIST1H2AK	8330	Histone cluster 1, H2ak	6	Down	12.0	2.5	–4.78	0.04
82	GP2	GP2	2813	Glycoprotein 2 (zymogen granule membrane)	16	Down	17.6	3.5	–5.08	0.02
83	NFIA	NFIA	4774	Nuclear factor I/A	1	Down	21.2	4.0	–5.28	0.04
84	CNTNAP2	CNTNAP2	26047	Contactin associated protein-like 2	7	Down	3.8	0.6	–5.79	0.007

Cut-off: fold change>2, *p*-value <0.5. LLID: Locus link ID.

Table III. *List of differentially expressed genes in HER2+ cells*.

N	Gene name	Illumina gene name	LLID	Full name	Chr	Exp_ status	Average (HER2+ control)	Average (HER2+ SH003)	Fold change	Paired *t*-test
1	SNORD3C	SNORD3C	780853	Small nucleolar RNA, C/D box 3C	17	Up	4.8	271.2	56.19	0.16
2	PHF2P1	DKFZP686A1627	266695	PHD finger protein 2 pseudogene 1	13	Up	1.4	8.7	6.18	0.04
3	HIST1H4B	HIST1H4B	8366	Histone cluster 1, H4b	6	Up	10.3	41.4	4.03	0.10
4	ZFAND2A	ZFAND2A	90637	Zinc finger, AN1-type domain 2A	7	Up	363.8	1,268.0	3.49	0.02
5	RIOK3	RIOK3	8780	RIO kinase 3 (yeast)	18	Up	144.9	488.1	3.37	0.03
6	SNORA33	SNORA33	594839	Small nucleolar RNA, H/ACA box 33	6	Up	37.8	124.2	3.28	0.12
7	IL20RB	IL20RB	53833	Interleukin 20 receptor beta	3	Up	18.2	53.5	2.94	0.24
8	C3orf78	SNHG8	440957	Chromosome 3 open reading frame 78	3	Up	100.6	290.1	2.89	0.11
9	HIST1H3A	HIST1H3A	8350	Histone cluster 1, H3a	6	Up	5.2	14.6	2.78	0.00008
10	ZNF581	ZNF581	51545	Zinc finger protein 581	19	Up	316.6	826.1	2.61	0.13
11	SNORD10	SNORD10	652966	Small nucleolar RNA, C/D box 10	17	Up	12.3	29.7	2.41	0.11
12	TTC39B	TTC39B	158219	Tetratricopeptide repeat domain 39B	9	Up	24.9	57.7	2.31	0.01
13	CDK7	CDK7	1022	Cyclin-dependent kinase 7	5	Up	557.5	1,283.3	2.30	0.03
14	DRD3	DRD3	1814	Dopamine receptor D3	3	Up	15.3	32.6	2.12	0.04
15	ZFP62	ZFP62	643836	Zinc finger protein 62 homolog (mouse)	5	Up	13.1	27.4	2.10	0.01
16	CCDC112	CCDC112	153733	Coiled-coil domain containing 112	5	Up	57.4	118.8	2.07	0.06
17	ABCB6	ABCB6	10058	ATP-binding cassette, sub-family B (MDR/TAP), member 6	2	Down	201.8	100.7	–2.00	0.05
18	CELSR2	CELSR2	1952	Cadherin, EGF LAG seven-pass G-type receptor 2 (flamingo homolog, Drosophila)	1	Down	82.9	41.2	–2.01	0.0001
19	HNRNPUL1	HNRPUL1	11100	Heterogeneous nuclear ribonucleoprotein U-like 1	19	Down	1,192.2	590.9	–2.02	0.04
20	GABPAP	GABPAP	8327	GA binding protein transcription factor, alpha subunit pseudogene	7	Down	24.7	11.5	–2.14	0.03
21	LRP5	LRP5	4041	Low density lipoprotein receptor-related protein 5	11	Down	249.0	109.4	–2.28	0.01
22	TMTC4	TMTC4	84899	Transmembrane and tetratricopeptide repeat containing 4	13	Down	62.0	24.2	–2.57	0.17
23	MARCH9	MARCH9	92979	Membrane-associated ring finger (C3HC4) 9	12	Down	22.1	7.3	–3.04	0.03
24	HOXA11-AS	HOXA11AS	221883	HOXA11 antisense RNA	7	Down	11.2	3.5	–3.23	0.02
25	MIR630	MIR630	693215	MicroRNA 630	15	Down	9.6	2.4	–3.98	0.06

Cut-off: fold change >2, *p*-value <0.5. LLID: Locus link ID.

Table IV. *List of differentially expressed genes in ER+ cells.*

N	Gene name	Illumina gene name	LLID	Full name	Chr	Exp_ status	Average (ER+ control)	Average (ER+ SH003)	Fold change	Paired *t*-test
1	FAM86EP	LOC348926	348926	Family with sequence similarity 86, member A pseudogene	4	Up	1.7	19.2	11.44	0.04
2	SESN2	SESN2	83667	Sestrin 2	1	Up	32.6	294.7	9.04	0.02
3	LOC649395	LOC649395	649395	Tyrosine 3-monooxygenase/tryptophan 5-monooxygenase activation protein, epsilon polypeptide pseudogene	7	Up	1.8	15.5	8.52	0.0002
4	NFKB2	NFKB2	4791	Nuclear factor of kappa light polypeptide gene enhancer in B-cells 2 (p49/p100)	10	Up	67.3	376.5	5.59	0.03
5	NLRP3	NLRP3	114548	NLR family, pyrin domain containing 3	1	Up	4.0	20.9	5.24	0.003
6	RNF19B	RNF19B	127544	Ring finger protein 19B	1	Up	85.4	431.2	5.05	0.02
7	LARP6	LARP6	55323	La ribonucleoprotein domain family, member 6	15	Up	47.4	228.2	4.81	0.02
8	REEP2	REEP2	51308	Receptor accessory protein 2	5	Up	0.9	4.4	4.63	0.02
9	ASNS	ASNS	440	Asparagine synthetase (glutamine-hydrolyzing)	7	Up	811.7	3,670.9	4.52	0.03
10	ZYX	ZYX	7791	Zyxin	7	Up	337.7	1523.8	4.51	0.03
11	ISG20	ISG20	3669	Interferon stimulated exonuclease gene 20kDa	15	Up	917.0	3,979.0	4.34	0.04
12	IFFO1	IFFO1	25900	Intermediate filament family orphan 1	12	Up	25.4	107.7	4.25	0.03
13	IFRD1	IFRD1	3475	Interferon-related developmental regulator 1	7	Up	132.6	556.0	4.19	0.04
14	RND3	RND3	390	Rho family GTPase 3	2	Up	232.6	931.8	4.01	0.001
15	SERTAD4-AS1	C1ORF133	574036	SERTAD4 antisense RNA 1	1	Up	93.1	362.3	3.89	0.02
16	LOC143666	LOC143666	143666	Uncharacterized LOC143666	11	Up	54.1	208.9	3.86	0.03
17	RNU12-2P	RNU12	26823	RNA, U12 small nuclear 2, pseudogene	X	Up	9.6	36.2	3.79	0.04
18	ZNF814	LOC730051	730051	Zinc finger protein 814	19	Up	7.1	26.4	3.71	0.01
19	HERC2P10	LOC390561	390561	Hect domain and RLD 2 pseudogene 10	15	Up	7.0	25.3	3.61	0.01
20	CIDECP	CIDECP	152302	Cell death-inducing DFFA-like effector c pseudogene	3	Up	31.7	114.1	3.60	0.01
21	GTPBP2	GTPBP2	54676	GTP binding protein 2	6	Up	29.6	106.1	3.59	0.05
22	NFIL3	NFIL3	4783	Nuclear factor, interleukin 3 regulated	9	Up	90.6	322.7	3.56	0.01
23	CSRP2	CSRP2	1466	Cysteine and glycine-rich protein 2	12	Up	162.6	562.4	3.46	0.02
24	SPRR2D	SPRR2D	6703	Small proline-rich protein 2D	1	Up	11.7	40.0	3.40	0.001
25	AEN	AEN	64782	Apoptosis enhancing nuclease	15	Up	287.5	952.2	3.31	0.04
26	MUS81	MUS81	80198	MUS81 endonuclease homolog (S. cerevisiae)	11	Up	265.0	859.2	3.24	0.008
27	RFPL4B	RFPL4B	442247	Ret finger protein-like 4B	6	Up	3.2	10.4	3.24	0.002
28	SLMO1	SLMO1	10650	Slowmo homolog 1 (Drosophila)	18	Up	56.7	183.7	3.24	0.006
29	C11orf9	C11ORF9	745	Chromosome 11 open reading frame 9	11	Up	5.2	16.3	3.12	0.02
30	ANKRD20A7P	LOC653436	653436	Ankyrin repeat domain 20 family, member A7, pseudogene	9	Up	5.3	16.5	3.10	0.0006
31	FRG2B	FRG2B	441581	FSHD region gene 2 family, member B	10	Up	5.0	15.3	3.06	0.03
32	STX1A	STX1A	6804	Syntaxin 1A (brain)	7	Up	126.3	366.0	2.90	0.03
33	BCL2A1	BCL2A1	597	BCL2-related protein A1	15	Up	4.7	13.6	2.88	0.04
34	SPRR2F	SPRR2F	6705	Small proline-rich protein 2F	1	Up	6.9	19.7	2.88	0.01
35	ZNF671	ZNF671	79891	Zinc finger protein 671	19	Up	5.1	14.6	2.88	0.01
36	LOC643634	LOC643634	643634	Tropomyosin 1 (alpha) pseudogene	3	Up	8.6	24.6	2.85	0.02
37	VPS53	VPS53	55275	Vacuolar protein sorting 53 homolog (S. cerevisiae)	17	Up	5.6	15.8	2.85	0.03
38	RIMKLB	FAM80B	57494	Ribosomal modification protein rimK-like family member B	12	Up	36.0	101.4	2.82	0.0002
39	TUBB2A	TUBB2A	7280	Tubulin, beta 2A class IIa	6	Up	269.6	758.9	2.82	0.01
40	KLF4	KLF4	9314	Kruppel-like factor 4 (gut)	9	Up	109.8	308.4	2.81	0.05
41	BIRC3	BIRC3	330	Baculoviral IAP repeat containing 3	11	Up	106.8	298.8	2.80	0.05
42	APOOL	APOOL	139322	Apolipoprotein O-like	X	Up	105.6	295.1	2.80	0.03

Table IV. *Continued*

Table IV. *List of differentially expressed genes in ER+ cells.*

N	Gene name	Illumina gene name	LLID	Full name	Chr	Exp_ status	Average (ER+ control)	Average (ER+ SH003)	Fold change	Paired *t*-test
43	TAF1D	TAF1D	79101	TATA box binding protein (TBP)-associated factor, RNA polymerase I, D, 41kDa	11	Up	26.5	73.4	2.77	0.02
44	BTBD17	BTBD17	388419	BTB (POZ) domain containing 17	17	Up	7.0	19.2	2.74	0.03
45	SNX8	SNX8	29886	Sorting nexin 8	7	Up	206.1	558.8	2.71	0.04
46	RAB3IL1	RAB3IL1	5866	RAB3A interacting protein (rabin3)-like 1	11	Up	207.6	562.6	2.71	0.007
47	MAFG	MAFG	4097	V-maf musculoaponeurotic fibrosarcoma oncogene homolog G (avian)	17	Up	71.2	188.2	2.65	0.04
48	POLR3C	POLR3C	10623	Polymerase (RNA) III (DNA directed) polypeptide C (62kD)	1	Up	547.8	1443.9	2.64	0.05
49	ALOXE3	ALOXE3	59344	Arachidonate lipoxygenase 3	17	Up	20.4	53.7	2.64	0.05
50	SOX11	SOX11	6664	SRY (sex determining region Y)-box 11	2	Up	4.7	12.5	2.63	0.02
51	TPCN1	TPCN1	53373	Two pore segment channel 1	12	Up	8.0	21.0	2.62	0.04
52	TXNL4B	TXNL4B	54957	Thioredoxin-like 4B	16	Up	28.7	75.2	2.62	0.01
53	LOC649133	LOC649133	649133	Uncharacterized LOC649133	11	Up	7.5	19.5	2.59	0.04
54	SLC30A1	SLC30A1	7779	Solute carrier family 30 (zinc transporter), member 1	1	Up	99.3	251.9	2.54	0.04
55	FAM167A	FAM167A	83648	Family with sequence similarity 167, member A	8	Up	38.6	96.8	2.51	0.02
56	NAPSB	NAPSB	256236	Napsin B aspartic peptidase, pseudogene	19	Up	6.1	15.2	2.51	0.04
57	LOC440900	LOC440900	440900	Uncharacterized LOC440900	2	Up	21.3	53.3	2.51	0.02
58	FAM13B	C5ORF5	51306	Family with sequence similarity 13, member B	5	Up	105.3	262.8	2.50	0.04
59	TTC21A	TTC21A	199223	Tetratricopeptide repeat domain 21A	3	Up	14.3	35.5	2.48	0.04
60	C6orf52	C6ORF52	347744	Chromosome 6 open reading frame 52	6	Up	28.9	71.3	2.47	0.05
61	LOC155060	LOC155060	155060	AI894139 pseudogene	7	Up	12.6	30.9	2.45	0.03
62	TMCC2	TMCC2	9911	Transmembrane and coiled-coil 2 domain family	1	Up	5.4	13.1	2.45	0.0009
63	HIST1H3D	HIST1H3D	8351	Histone cluster 1, H3d	6	Up	30.8	75.2	2.44	0.02
64	ZFAND2A	ZFAND2A	90637	Zinc finger, AN1-type domain 2A	7	Up	468.2	1120.8	2.39	0.001
65	SLC7A5P1	SLC7A5P1	81893	Solute carrier family 7 (amino acid transporter light chain, L system), member 5 pseudogene 1	16	Up	13.2	31.5	2.39	0.05
66	LOC727751	LOC727751	727751	Uncharacterized LOC727751	15	Up	20.9	49.3	2.36	0.0004
67	KLC3	KLC3	147700	Kinesin light chain 3	19	Up	11.8	27.8	2.36	0.008
68	RFESD	RFESD	317671	Rieske (Fe-S) domain containing	5	Up	45.4	106.1	2.34	0.04
69	MIR22HG	C17ORF91	84981	MIR22 host gene (non-protein coding)	17	Up	52.9	123.1	2.33	0.005
70	PQLC2	PQLC2	54896	PQ loop repeat containing 2	1	Up	14.7	34.0	2.31	0.02
71	LOC286135	LOC286135	286135	Uncharacterized LOC286135	8	Up	10.9	25.2	2.30	0.05
72	RSPH3	RSPH3	83861	Radial spoke 3 homolog (Chlamydomonas)	6	Up	70.2	160.7	2.29	0.04
73	RRNAD1	C1ORF66	51093	Ribosomal RNA adenine dimethylase domain containing 1	1	Up	160.8	363.2	2.26	0.03
74	DUSP10	DUSP10	11221	Dual specificity phosphatase 10	1	Up	25.9	57.8	2.23	0.04
75	PIGA	PIGA	5277	Phosphatidylinositol glycan anchor biosynthesis, class A	X	Up	122.4	272.6	2.23	0.003
76	LOC643219	LOC643219	643219	Glycerol-3-phosphate acyltransferase 2, mitochondrial pseudogene	2	Up	5.9	13.1	2.21	0.003
77	TFE3	TFE3	7030	Transcription factor binding to IGHM enhancer 3	X	Up	62.5	136.3	2.18	0.006
78	GPS2	GPS2	2874	G protein pathway suppressor 2	17	Up	152.8	332.8	2.18	0.05
79	TGIF1	TGIF1	7050	TGFB-induced factor homeobox 1	18	Up	142.8	308.4	2.16	0.02
80	SLC3A2	SLC3A2	6520	Solute carrier family 3 (activators of dibasic and neutral amino acid transport), member 2	11	Up	944.8	2032.7	2.15	0.02

Table IV. *Continued*

Table IV. *Continued*

N	Gene name	Illumina gene name	LLID	Full name	Chr	Exp_ status	Average (ER+ control)	Average (ER+ SH003)	Fold change	Paired *t*-test
81	MCL1	MCL1	4170	Myeloid cell leukemia sequence 1 (BCL2-related)	1	Up	250.4	532.3	2.13	0.03
82	TPM4	TPM4	7171	Tropomyosin 4	19	Up	168.3	355.6	2.11	0.01
83	PHLDB3	LOC653583	653583	Pleckstrin homology-like domain, family B, member 3	19	Up	60.3	126.7	2.10	0.04
84	CCDC50	CCDC50	152137	Coiled-coil domain containing 50	3	Up	179.6	376.4	2.10	0.05
85	IGSF21	IGSF21	84966	Immunoglobin superfamily, member 21	1	Up	2.2	4.7	2.09	0.03
86	PTCHD2	PTCHD2	57540	Patched domain containing 2	1	Up	15.7	32.8	2.09	0.01
87	CHGA	CHGA	1113	Chromogranin A (parathyroid secretory protein 1)	14	Up	16.8	35.1	2.09	0.03
88	ISL2	ISL2	64843	ISL LIM homeobox 2	15	Up	19.2	39.9	2.08	0.03
89	PMM1	PMM1	5372	Phosphomannomutase 1	22	Up	234.8	487.1	2.07	0.02
90	ABL2	ABL2	27	V-abl Abelson murine leukemia viral oncogene homolog 2	1	Up	16.1	33.4	2.07	0.03
91	ARSK	ARSK	153642	Arylsulfatase family, member K	5	Up	18.7	38.6	2.06	0.004
92	IQCA1P1	LOC392843	392843	IQ motif containing with AAA domain 1 pseudogene 1	7	Up	6.2	12.8	2.06	0.01
93	HES4	HES4	57801	Hairy and enhancer of split 4 (Drosophila)	1	Up	1,613.3	3271.6	2.03	0.03
94	C18orf21	C18ORF21	83608	Chromosome 18 open reading frame 21	18	Up	195.2	395.9	2.03	0.02
95	DYRK4	DYRK4	8798	Dual-specificity tyrosine-(Y)-phosphorylation regulated kinase 4	12	Up	272.5	551.6	2.02	0.04
96	STYXL1	STYXL1	51657	Serine/threonine/tyrosine interacting-like 1	7	Up	588.0	1186.7	2.02	0.02
97	NGLY1	NGLY1	55768	N-glycanase 1	3	Up	238.9	481.2	2.01	0.01
98	SNHG7	SNHG7	84973	Small nucleolar RNA host gene 7 (non-protein coding)	9	Up	507.6	1018.4	2.01	0.04
99	RTN4IP1	RTN4IP1	84816	Reticulon 4 interacting protein 1	6	Down	184.4	92.1	–2.00	0.04
100	TMEM123	TMEM123	114908	Transmembrane protein 123	11	Down	731.7	365.0	–2.00	0.04
101	IMPAD1	IMPAD1	54928	Inositol monophosphatase domain containing 1	8	Down	233.4	116.2	–2.01	0.04
102	LSM14A	LSM14A	26065	LSM14A, SCD6 homolog A (S. cerevisiae)	19	Down	427.2	212.6	–2.01	0.02
103	KDELR1	KDELR1	10945	KDEL (Lys-Asp-Glu-Leu) endoplasmic reticulum protein retention receptor 1	19	Down	1,688.9	839.6	–2.01	0.02
104	PCMTD2	PCMTD2	55251	Protein-L-isoaspartate (D-aspartate) O-methyltransferase domain containing 2	20	Down	173.5	86.1	–2.01	0.04
105	CHD4	CHD4	1108	Chromodomain helicase DNA binding protein 4	12	Down	750.7	372.7	–2.01	0.03
106	TTF2	TTF2	8458	Transcription termination factor, RNA polymerase II	1	Down	418.3	206.5	–2.03	0.02
107	SNRPD1	SNRPD1	6632	Small nuclear ribonucleoprotein D1 polypeptide 16kDa	18	Down	143.6	70.7	–2.03	0.002
108	STAU2	STAU2	27067	Staufen, RNA binding protein, homolog 2 (Drosophila)	8	Down	133.4	65.4	–2.04	0.02
109	INSL5	INSL5	10022	Insulin-like 5	1	Down	33.7	16.5	–2.05	0.03
110	LINC00085	NCRNA00085	147650	Long intergenic non-protein coding RNA 85	19	Down	148.3	72.5	–2.05	0.03
111	MTCH2	MTCH2	23788	Mitochondrial carrier 2	11	Down	82.5	40.2	–2.05	0.05
112	RBMX	RBMX	27316	RNA binding motif protein, X-linked	X	Down	609.7	297.0	–2.05	0.04
113	EPSTI1	EPSTI1	94240	Epithelial stromal interaction 1 (breast)	13	Down	22.3	10.8	–2.06	0.04
114	DHCR24	DHCR24	1718	24-dehydrocholesterol reductase	1	Down	553.1	266.1	–2.08	0.009
115	PIK3CB	PIK3CB	5291	Phosphatidylinositol-4,5-bisphosphate 3-kinase, catalytic subunit beta	3	Down	83.0	39.8	–2.09	0.03

Table IV. *Continued*

Table IV. *Continued*

N	Gene name	Illumina gene name	LLID	Full name	Chr	Exp_ status	Average (ER+ control)	Average (ER+ SH003)	Fold change	Paired *t*-test
116	HNRNPUL1	HNRPUL1	11100	Heterogeneous nuclear ribonucleoprotein U-like 1	19	Down	974.5	464.5	–2.10	0.02
117	KLF9	KLF9	687	Kruppel-like factor 9	9	Down	168.1	79.8	–2.11	0.02
118	CFP	CFP	5199	Complement factor properdin	X	Down	16.0	7.6	–2.12	0.02
119	LRRC16A	LRRC16	55604	Leucine rich repeat containing 16A	6	Down	64.5	30.2	–2.14	0.04
120	VOPP1	ECOP	81552	Vesicular, overexpressed in cancer, prosurvival protein 1	7	Down	150.8	70.6	–2.14	0.009
121	HPSE	HPSE	10855	Heparanase	4	Down	36.5	17.1	–2.14	0.003
122	FAM20B	FAM20B	9917	Family with sequence similarity 20, member B	1	Down	997.0	464.6	–2.15	0.01
123	ARF3	ARF3	377	ADP-ribosylation factor 3	12	Down	934.9	435.2	–2.15	0.04
124	LOC100131735	LOC100131735	100131735	RNA-binding motif protein, X chromosome-like	9	Down	513.4	238.1	–2.16	0.04
125	SUMO2P3	LOC652489	652489	SMT3 suppressor of mif two 3 homolog 2 (S. cerevisiae) pseudogene 3	7	Down	822.4	380.5	–2.16	0.04
126	GPD1L	GPD1L	23171	Glycerol-3-phosphate dehydrogenase 1-like	3	Down	1,019.8	471.7	–2.16	0.05
127	ICMT	ICMT	23463	Isoprenylcysteine carboxyl methyltransferase	1	Down	363.7	167.9	–2.17	0.04
128	NUP210	NUP210	23225	Nucleoporin 210kDa	3	Down	264.7	122.1	–2.17	0.04
129	PTBP3	ROD1	9991	Polypyrimidine tract binding protein 3	9	Down	759.8	349.9	–2.17	0.02
130	LINC00094	NCRNA00094	266655	Long intergenic non-protein coding RNA 94	9	Down	96.2	44.2	–2.18	0.04
131	VMA21	LOC203547	203547	VMA21 vacuolar H+-ATPase homolog (S. cerevisiae)	X	Down	392.3	180.1	–2.18	0.02
132	RFX5	RFX5	5993	Regulatory factor X, 5 (influences HLA class II expression)	1	Down	407.8	187.1	–2.18	0.009
133	LDLRAD1	LDLRAD1	388633	Low density lipoprotein receptor class A domain containing 1	1	Down	15.4	7.1	–2.18	0.02
134	ELOVL6	ELOVL6	79071	ELOVL fatty acid elongase 6	4	Down	169.4	77.4	–2.19	0.02
135	MANEA	MANEA	79694	Mannosidase, endo-alpha	6	Down	17.3	7.9	–2.20	0.04
136	TSPYL4	TSPYL4	23270	TSPY-like 4	6	Down	39.1	17.7	–2.21	0.05
137	ADCY9	ADCY9	115	Adenylate cyclase 9	16	Down	112.6	50.9	–2.21	0.005
138	CDHR2	PCDH24	54825	Cadherin-related family member 2	5	Down	31.1	14.0	–2.23	0.02
139	SUMF1	SUMF1	285362	Sulfatase modifying factor 1	3	Down	483.9	215.8	–2.24	0.04
140	KBTBD4	KBTBD4	55709	Kelch repeat and BTB (POZ) domain containing 4	11	Down	239.9	106.6	–2.25	0.001
141	MAST3	MAST3	23031	Microtubule associated 3 serine/threonine kinase	19	Down	71.5	31.7	–2.25	0.02
142	KITLG	KITLG	4254	KIT ligand	12	Down	57.1	25.3	–2.26	0.02
143	CTXN1	CTXN1	404217	Cortexin 1	19	Down	1,581.1	697.6	–2.27	0.04
144	LPHN1	LPHN1	22859	Latrophilin 1	19	Down	106.6	46.5	–2.29	0.04
145	KIAA1161	KIAA1161	57462	KIAA1161	9	Down	54.5	23.4	–2.33	0.02
146	HCFC1	HCFC1	3054	Host cell factor C1 (VP16-accessory protein)	X	Down	773.5	331.9	–2.33	0.04
147	PRDX3	PRDX3	10935	Peroxiredoxin 3	10	Down	1,959.9	840.2	–2.33	0.01
148	FASN	FASN	2194	Fatty acid synthase	17	Down	6,552.1	2744.1	–2.39	0.007
149	SRD5A3	SRD5A3	79644	Steroid 5 alpha-reductase 3	4	Down	21.9	9.1	–2.40	0.006
150	PTMAP8	LOC728873	728873	Prothymosin, alpha pseudogene 8	3	Down	4177.5	1728.2	–2.42	0.04
151	BAG1	BAG1	573	BCL2-associated athanogene	9	Down	51.1	21.1	–2.43	0.001
152	TUBB	TUBB	203068	Tubulin, beta class I	6	Down	2,054.4	842.8	–2.44	0.02
153	SHROOM3	SHROOM3	57619	Shroom family member 3	4	Down	76.6	31.0	–2.47	0.01
154	LOC730246	LOC730246	730246	Heterogeneous nuclear ribonucleoprotein A1 pseudogene	1	Down	4,504.0	1,806.2	–2.49	0.002

Table IV. *Continued*

Table IV. *Continued*

N	Gene name	Illumina gene name	LLID	Full name	Chr	Exp_ status	Average (ER+ control)	Average (ER+ SH003)	Fold change	Paired *t*-test
155	XRCC5	XRCC5	7520	X-ray repair complementing defective repair in Chinese hamster cells 5 (double-strand-break rejoining)	2	Down	436.1	174.8	–2.50	0.008
156	RIMS3	RIMS3	9783	Regulating synaptic membrane exocytosis 3	1	Down	53.6	21.4	–2.50	0.01
157	SCARNA23	SCARNA23	677773	Small Cajal body-specific RNA 23	X	Down	10.7	4.2	–2.54	0.005
158	ESX1	ESX1	80712	ESX homeobox 1	X	Down	14.0	5.5	–2.54	0.006
159	ATP6V0A1	ATP6V0A1	535	ATPase, H+ transporting, lysosomal V0 subunit a1	17	Down	537.6	211.4	–2.54	0.04
160	TMEM30A	TMEM30A	55754	Transmembrane protein 30A	6	Down	122.7	47.8	–2.57	0.01
161	SCD	SCD	6319	Stearoyl-CoA desaturase (delta-9-desaturase)	10	Down	3,882.1	1438.5	–2.70	0.04
162	NUDT21	NUDT21	11051	Nudix (nucleoside diphosphate linked moiety X)-type motif 21	16	Down	128.2	47.4	–2.70	0.04
163	EFCAB3	EFCAB3	146779	EF-hand calcium binding domain 3	17	Down	13.2	4.9	–2.72	0.02
164	SFXN1	SFXN1	94081	Sideroflexin 1	5	Down	158.3	56.7	–2.79	0.05
165	SUOX	SUOX	6821	Sulfite oxidase	12	Down	150.7	52.6	–2.87	0.01
166	RAB40B	RAB40B	10966	RAB40B, member RAS oncogene family	17	Down	322.8	112.3	–2.87	0.01
167	CELSR2	CELSR2	1952	Cadherin, EGF LAG seven-pass G-type receptor 2 (flamingo homolog, Drosophila)	1	Down	208.4	69.0	–3.02	0.03
168	SCDP1	LOC645313	645313	Stearoyl-CoA desaturase (delta-9-desaturase) pseudogene 1	17	Down	57.1	18.8	–3.03	0.003
169	LOC645691	LOC645691	645691	Heterogeneous nuclear ribonucleoprotein A1 pseudogene	2	Down	280.2	92.1	–3.04	0.05
170	FAM122B	FAM122B	159090	Family with sequence similarity 122B	X	Down	167.7	51.4	–3.27	0.008
171	DARS2	DARS2	55157	Aspartyl-tRNA synthetase 2, mitochondrial	1	Down	258.3	79.0	–3.27	0.005
172	LOC728643	LOC728643	728643	Heterogeneous nuclear ribonucleoprotein A1 pseudogene	10	Down	1,443.6	388.1	–3.72	0.03
173	SNORA56	SNORA56	677835	Small nucleolar RNA, H/ACA box 56	X	Down	20.0	5.4	–3.73	0.005
174	RAB26	RAB26	25837	RAB26, member RAS oncogene family	16	Down	386.1	92.9	–4.16	0.009

Cut-off: fold change>2, *p*-value <0.5. LLID: Locus link ID.

stress. Therefore, we further examined this possibility. We found that SH003 increased the protein expression levels of BIP and CHOP, and phosphorylation levels of PERK, eIF2α, IRE1α and JNK, independently of the subtype of breast cancer cells (Figure 3A). To confirm that SH003 causes ER stress-induced apoptosis, HCC-1419 (HER2-positive), MCF-7 (ER-positive) and MDA-MB-231 (triple-negative) breast cancer cells were pretreated with an inhibitor of ER stress pathway (4-PBA) for 2 h, and then treated with SH003 for another 24 h. 4-PBA reduced levels of BIP, CHOP, cleaved Caspase-7 and cleaved PARP increased by SH003 (Figure 3B), suggesting that SH003 could cause apoptosis of breast cancer cells *via* ER stress. Consistently, 4-PBA reduced SH003-increased apoptotic cell number (Figure 3C). Therefore, SH003 causes apoptosis *via* ER stress, independently of the subtype of breast cancer cells.

SH003 causes ER stress via the increase of intracellular ROS level in breast cancer cell lines. Increase of intracellular reactive oxygen species (ROS) level results in ER stress followed by apoptosis and *vice versa* (33, 34). Moreover, we recently found that SH003 induces intracellular ROS production in MDA-MB-231 cells (11). Therefore, we examined whether SH003 commonly causes an increase of intracellular ROS level in breast cancer cell lines. HCC-1419, MCF-7 and MDA-MB-231 breast cancer cells were pretreated with NAC, an inhibitor of ROS production, for 30 min followed by SH003 treatment for another 4 h. SH003 significantly increased intracellular ROS level independently of breast cancer subtype, and NAC failed to reduce SH003-induced intracellular ROS production (Figure 4A), suggesting that SH003 might overcome NAC inhibition of ROS

Table V. *Candidate enriched gene sets for the differentially expressed genes in breast cancer cells.*

Group	Gene expression	Category	Gene ontology category	Number of reference genes in the category	Observed gene number	Expected gene number	Ratio of enrichment	Significance of enrichment ($p$corr<0.05)	Significance of enrichment (raw p-Value)	Observed genes
All: SH003 *vs*. control	Up-regulation	Biological process	Response to unfolded protein	121	6	0.57	10.49	0.02	0.000022	ATF3, HSPA7, CHAC1, PPP1R15A, DDIT3, DNAJB9
			Response to topologically incorrect protein	128	6	0.6	9.92	0.02	0.00003	ATF3, HSPA7, CHAC1, PPP1R15A, DDIT3, DNAJB9
			Regulation of macromolecule metabolic process	3,833	33	18.12	1.82	0.05	0.000066	HABP4, SERTAD1, PAWR, CHAC1, HMOX1, GABPB1, DUSP5, DNAJB9, BLOC1S2, SOCS1, FOSB, FEM1B, POLR3C, ZNF460, NKX2-1, DUSP1, ZNF184, ELL2, NR1H4, RGCC, ATF3, KDM3A, FOS, DAPK3, PPP1R15A, WWTR1, NFIL3, GADD45B, CEBPG, EID3, SAMD8, CCRN4L, DDIT3
		Molecular function	Transcription corepressor	178	6	0.78	7.65	0.01	0.0001	ATF3, PAWR, NR1H4, DDIT3, NFIL3, WWTR1
			activity protein dimerization activity	902	13	3.97	3.27	0.01	0.0001	GCLM, STX1A, HIST1H2BN, NFIL3, WWTR1, FOSB, CEBPG, ATF3, HMOX1, FOS, GABPB1, DDIT3, DAPK3
			Calcium channel inhibitor activity	4	2	0.02	113.52	0.01	0.0001	SLC30A1, STX1A
			Thyroid hormone receptor activity	7	2	0.03	64.87	0.05	0.0004	NR1H4, NR4A3
			Leucine zipper domain binding	7	2	0.03	64.87	0.05	0.0004	PAWR, DAPK3
		Cellular component	Nucleus	5,408	45	24.37	1.85	3.1E-05	0.00000039	HABP4, PAWR, TXNL4B, HMOX1, GABPB1, BEX2, DUSP5, DNAJB9, BLOC1S2, ZYX, ZFAND2A, SOCS1, FOSB, FEM1B, INTS12, C12orf39, POLR3C, ZNF460, C2CD4B, DUSP1, NKX2-1, IFRD1, ZNF184, SESN2, HIST1H2BN, ELL2, NR1H4, ZMYM5, RGCC, HSPA7, ATF3, KDM3A, FOS, DAPK3, MUS81, NFIL3, GADD45B, WWTR1, CEBPG, NR4A3, EID3, CCNB1IP1, CCRN4L, DDIT3, HIST1H1C

Table V. *Continued*

Table V. *Continued*

Group	Gene expression	Category	Gene ontology category	Number of reference genes in the category	Observed gene number	Expected gene number	Ratio of enrichment	Significance of enrichment ($p$corr<0.05)	Significance of enrichment (raw p-Value)	Observed genes
			Intracellular membrane-bounded organelle	8,740	55	39.38	1.4	0.005	0.000064	HABP4, PAWR, CHAC1, TXNL4B, HMOX1, GABPB1, BEX2, DUSP5, DNAJB9, BLOC1S2, ZYX, ZFAND2A, SOCS1, FOSB, FEM1B, INTS12, C12orf39, POLR3C, ZNF460, C2CD4B, SLMO1, DUSP1, NKX2-1, ZNF184, IFRD1, SLC3A2, SESN2, ELL2, HIST1H2BN, NR1H4, ZMYM5, RGCC, HSPA7, ATF3, KDM3A, C3orf78, FOS, NEU1, DAPK3, MUS81, STX1A, RND3, PPP1R15A, NFIL3, WWTR1, GADD45B, CEBPG, NR4A3, EID3, SAMD8, ARC, CCNB1IP1, CCRN4L, DDIT3, HIST1H1C
			Membrane-bounded organelle	8,750	55	39.42	1.4	0.005	0.000066	HABP4, PAWR, CHAC1, TXNL4B, HMOX1, GABPB1, BEX2, DUSP5, DNAJB9, BLOC1S2, ZYX, ZFAND2A, SOCS1, FOSB, FEM1B, INTS12, C12orf39, POLR3C, ZNF460, C2CD4B, SLMO1, DUSP1, NKX2-1, ZNF184, IFRD1, SLC3A2, SESN2, ELL2, HIST1H2BN, NR1H4, ZMYM5, RGCC, HSPA7, ATF3, KDM3A, C3orf78, FOS, NEU1, DAPK3, MUS81, STX1A, RND3, PPP1R15A, NFIL3, WWTR1, GADD45B, CEBPG, NR4A3, EID3, SAMD8, ARC, CCNB1IP1, CCRN4L, DDIT3, HIST1H1C
			Intracellular part	11,149	62	50.23	1.23	0.04	0.0005	GCLM, HABP4, PAWR, CHAC1, TXNL4B, C2orf49, HMOX1, GABPB1, BEX2, DUSP5, DNAJB9, SRXN1, BLOC1S2, ZYX, ZFAND2A, SOCS1, FOSB, FEM1B, INTS12, C12orf39, POLR3C, ZNF460, C2CD4B, SLMO1, DUSP1, NKX2-1, ZNF184, IFRD1, SLC3A2, SESN2, ELL2, HIST1H2BN, NR1H4, ZMYM5, SAT1, GPCPD1, RGCC, HSPA7, ATF3, KDM3A, C3orf78, FOS, NEU1, DAPK3, RIMKLB, MUS81, STX1A, RND3, PPP1R15A, HSPBAP1, NFIL3, WWTR1,

Table V. *Continued*

Table V. *Continued*

Group	Gene expression	Category	Gene ontology category	Number of reference genes in the category	Observed gene number	Expected gene number	Ratio of enrichment	Significance of enrichment ($p$corr<0.05)	Significance of enrichment (raw p-Value)	Observed genes
										GADD45B, CEBPG, NR4A3, EID3, SAMD8, ARC, CCNB1IP1, CCRN4L, DDIT3, HIST1H1C
	Down-regulation	Biological process	No significant category detected	.	.	.	.	.	.	.
		Molecular function	Receptor tyrosine kinase binding	33	2	0.05	39.97	0.05	0.0011	PTPRF, PIK3R2
		Cellular component	No significant category detected	.	.	.	.	.	.	.
TNBC: SH003 *vs*. control	Up-regulation		No significant category detected	.	.	.	.	.	.	.
	Down-regulation		No significant category detected	.	.	.	.	.	.	.
HER2+: SH003 *vs*. control	Up-regulation		No significant category detected	.	.	.	.	.	.	.
	Down-regulation		No significant category detected	.	.	.	.	.	.	.
ER+: SH003 *vs*. control	Up-regulation	Biological process	No significant category detected	.	.	.	.	.	.	.
		Molecular function	Calcium channel inhibitor activity	4	2	0.02	119.39	0.01	0.0001	SLC30A1, STX1A

Table V. *Continued*

Table V. *Continued*

Group	Gene expression	Category	Gene ontology category	Number of reference genes in the category	Observed gene number	Expected gene number	Ratio of enrichment	Significance of enrichment ($p$corr<0.05)	Significance of enrichment (raw p-Value)	Observed genes
		Cellular component	No significant category detected	.	.	.	.	.	.	.
	Down-regulation	Biological process	No significant category detected	.	.	.	.	.	.	.
		Molecular function	Oxidoreductase activity, acting on the CH-CH group of donors, NAD or NADP as acceptor	20	3	0.08	39.95	0.006	0.000054	SRD5A3, DHCR24, FASN
		Molecular function	Protein carboxyl O-methyltransferase activity	5	2	0.02	106.53	0.01	0.0001	PCMTD2, ICMT
		Molecular function	Carboxyl-O-methyltransferase activity	5	2	0.02	106.53	0.01	0.0001	PCMTD2, ICMT
		Molecular function	Fatty acid synthase activity	8	2	0.03	66.58	0.04	0.0004	ELOVL6, FASN
		Cellular component	No significant category detected	.	.	.	.	.	.	.

Table VI. *Biological pathway analysis of differentially expressed genes.*

Group	Pathway name	#Genes in pathway	#Input genes in pathway	#Pathway genes on Chip	Genes	Impact factor	Corrected *p*-value	Corrected gamma *p*-value
All: SH003 *vs*. control	Phosphatidylinositol signaling system	76	1	76	PIK3R2	27.7	0.34	0.000000000026
	MAPK signaling pathway	272	7	266	AKT2, DDIT3, DUSP1, DUSP5, FOS, GADD45B, HSPA6	12.0	0.00068	0.000077
	Colorectal cancer	84	5	83	AKT2, BCL2, FOS, FZD4, PIK3R2	11.5	0.000095	0.00013
	Adherens junction	78	1	75	PTPRF	9.0	0.34	0.001
	Pathways in cancer	330	6	328	AKT2, BCL2, DAPK3, FOS, FZD4, PIK3R2	7.5	0.01	0.005
	B cell receptor signaling pathway	65	3	65	AKT2, FOS, PIK3R2	7.0	0.005	0.007
	Antigen processing and presentation	89	1	81	HSPA6	7.0	0.36	0.007
	Insulin signaling pathway	138	4	137	HSPA6AKT2, PIK3R2, PTPRF, SOCS1	6.5	0.007	0.01
	p53 signaling pathway	69	3	69	GADD45B, RRM2, SESN2	6.4	0.006	0.01
	T cell receptor signaling pathway	108	3	108	AKT2, FOS, PIK3R2	5.9	0.02	0.02
	Small cell lung cancer	86	3	85	AKT2, BCL2, PIK3R2	5.8	0.01	0.02
	Apoptosis	89	3	89	AKT2, BCL2, PIK3R2	5.7	0.01	0.02
	mTOR signaling pathway	52	2	51	AKT2, PIK3R2	5.6	0.03	0.02
	Jak-STAT signaling pathway	155	4	153	AKT2, IL20RB, PIK3R2, SOCS1	5.5	0.01	0.03
	Prostate cancer	90	3	89	AKT2, BCL2, PIK3R2	5.5	0.01	0.03
	Toll-like receptor signaling pathway	102	3	102	AKT2, FOS, PIK3R2	5.4	0.02	0.03
	Type II diabetes mellitus	45	2	43	PIK3R2, SOCS1	5.3	0.02	0.03
	Focal adhesion	203	4	199	AKT2, BCL2, PIK3R2, ZYX	5.1	0.02	0.04
	Basal cell carcinoma	55	1	55	FZD4	5.0	0.26	0.04
	Acute myeloid leukemia	59	2	57	AKT2, PIK3R2	4.7	0.04	0.05
TNBC: SH003 *vs*. control	Melanoma	71	2	71	AKT2, FGF19	7.2	0.02	0.006
	Pathways in cancer	330	2	328	AKT2, FGF19	4.9	0.30	0.04
HER2+: SH003 *vs*. control	Systemic lupus erythematosus	144	2	131	HIST1H3A, HIST1H4B	5.6	0.007	0.02
ER+: SH003 *vs*. control	Phosphatidylinositol signaling system	76	1	76	PIK3CB	33.3	0.41	0.00000000000012
	Vibrio cholerae infection	62	3	59	ADCY9, ATP6V0A1, KDELR1	5.7	0.008	0.02
	Biosynthesis of unsaturated fatty acids	22	2	22	ELOVL6, SCD	5.5	0.01	0.03
	Gap junction	96	3	96	ADCY9, TUBB, TUBB2A	5.4	0.03	0.03
	Apoptosis	89	2	89	BIRC3, PIK3CB	4.9	0.13	0.04

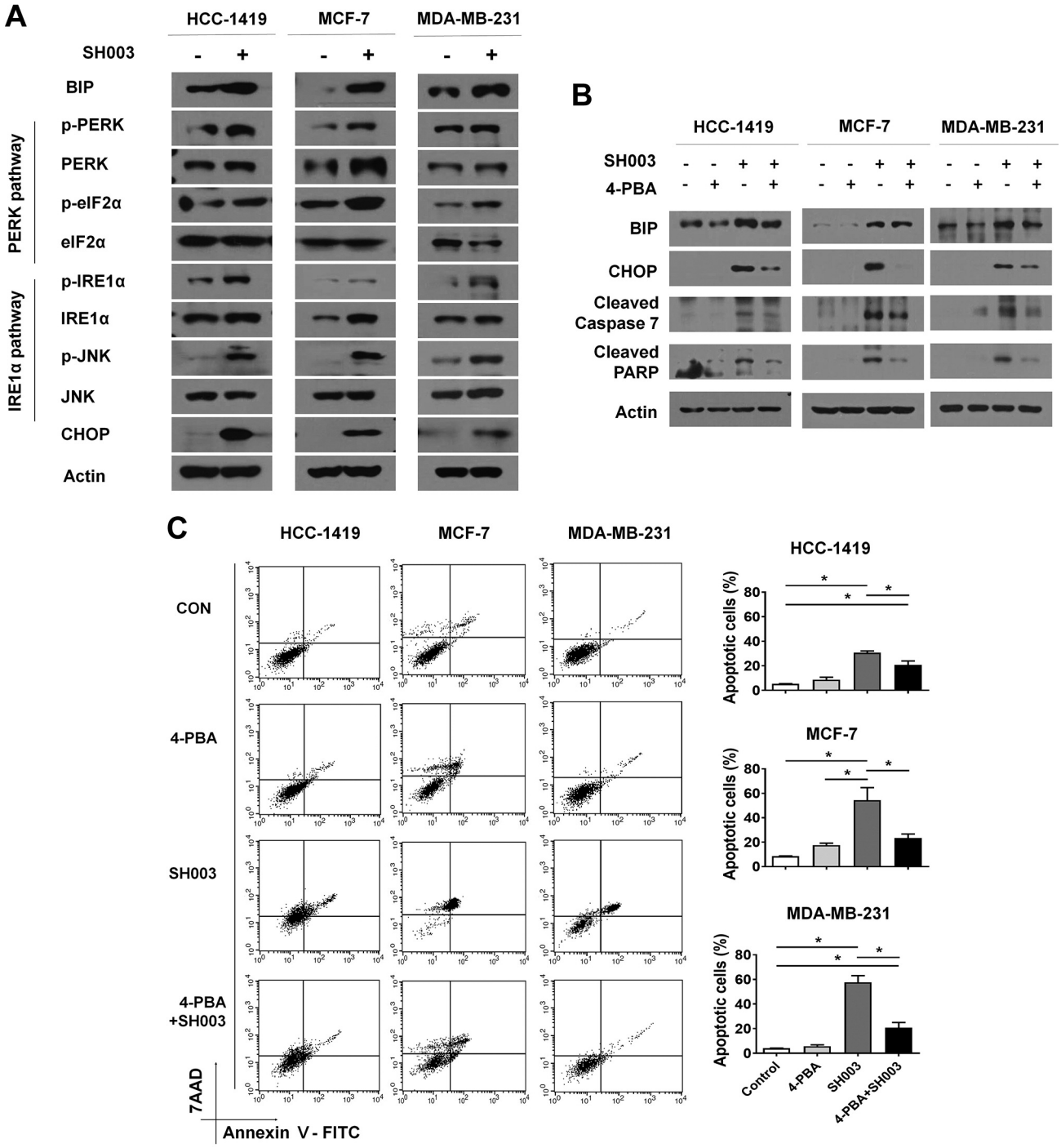

Figure 3. *SH003 causes apoptosis of breast cancer cells through ER stress. (A) SH003 induces ER stress in breast cancer cells. The cells were treated with SH003 at 500 μg/ml for 24 h. Protein levels of binding immunoglobulin protein (BIP), p-PKR-like endoplasmic reticulum kinase (PERK), PKR-like endoplasmic reticulum kinase (PERK), p-eukaryotic translation initiation factor 2A (eIF2α), eukaryotic translation initiation factor 2A (eIF2α), p-inositol-requiring enzyme 1α (IRE1α), inositol-requiring enzyme 1α (IRE1α), p-c-Jun n-terminal kinase (JNK), c-Jun n-terminal kinase (JNK) and C/EBP homologous protein (CHOP) were examined by western blot. Actin was detected as the internal loading control. (B) SH003-induced endoplasmic reticulum (ER) stress results in apoptotic cell death. The cells were pretreated with 4-PBA at 1 mM for 2 h and then treated with SH003 at 500 μg/ml for another 24 h. Protein levels of BIP, CHOP, cleaved Caspase-7 and cleaved PARP were examined by western blot. (C) Apoptotic cell death was confirmed by Annexin V-FITC and 7-AAD double-staining assay. The cells were pretreated with 4-Phenylbutyric acid (4-PBA) at 1 mM for 2 h and then treated with SH003 at 500 μg/ml for another 24 h. Bar graphs presented as mean and standard deviation indicate apoptotic cell numbers. *p<0.05. One-way ANOVA followed by the Bonferroni post hoc test.*

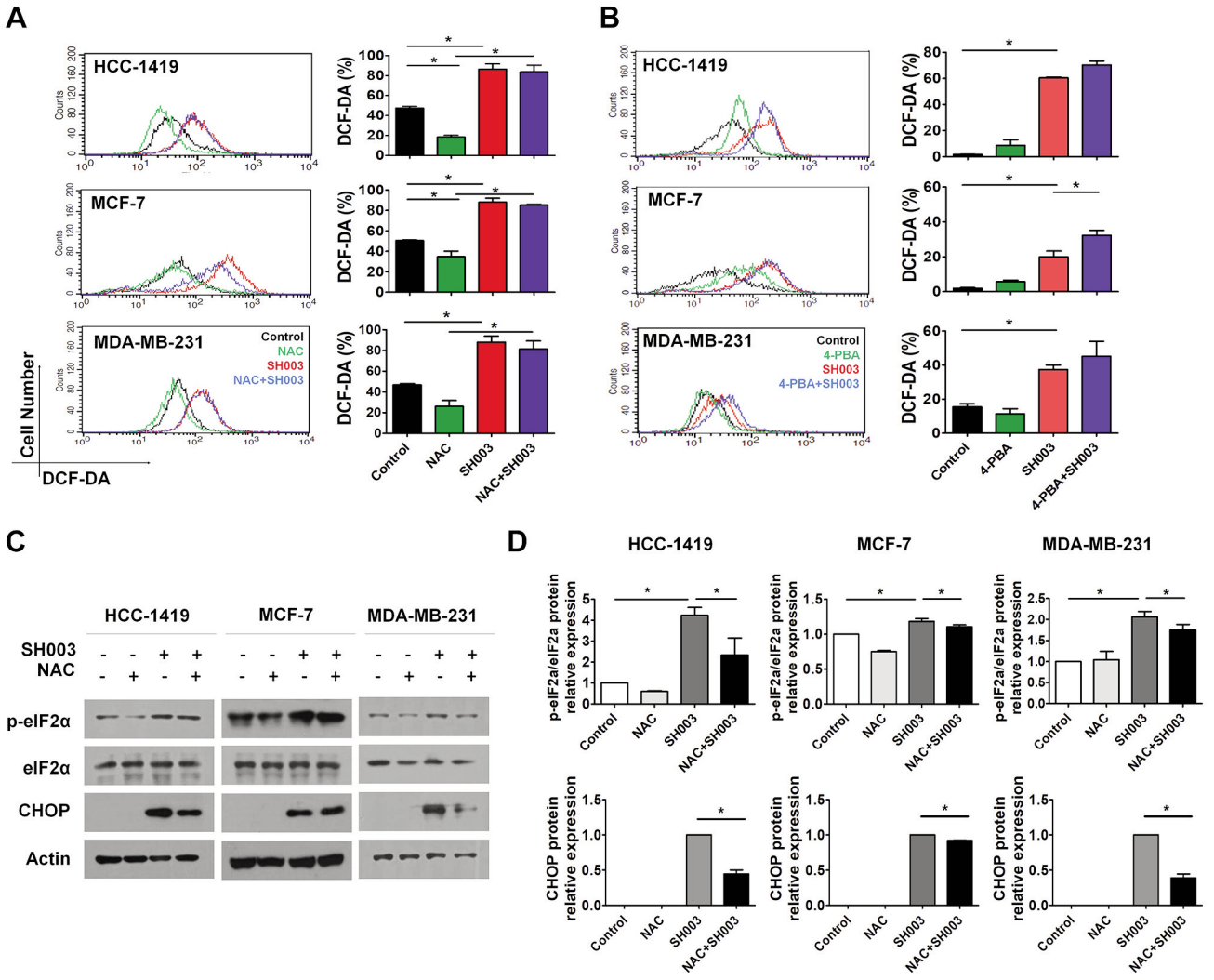

Figure 4. *SH003-induced ROS production results in ER stress. (A) SH003 increases intracellular reactive oxygen species (ROS) production. Breast cancer cells were pretreated with N-acetyl cysteine (NAC) at 5 mM for 30 min and then treated with SH003 at 500 μg/ml for 4 h. Intracellular ROS levels were measured by DCF-DA staining assay. Bar graphs indicating mean and standard deviation from three independent experiments show intracellular ROS levels. (B) SH003-increased ROS levels are accumulated by blocking ER stress. Breast cancer cells were pretreated with 4-PBA at 1 mM for 2 h and then treated with SH003 at 500 μg/ml for 4 h. Intracellular ROS levels were measured by DCF-DA staining assay. Bar graphs indicating mean and standard deviation from three independent experiments show intracellular ROS levels. (C) Inhibition of intracellular ROS production ameliorates SH003-induced ER stress. Protein levels of p-eIF2α, eIF2α and CHOP were examined by western blot. (D) Relative levels of p-eIF2α, eIF2α and CHOP. Bar graphs indicate mean and standard deviation. *p<0.05. One-way ANOVA followed by the Bonferroni post hoc test.*

production. However, 4-PBA rather slightly increased intracellular ROS production even under SH003 treatment (Figure 4B). Those data suggested that the intracellular ROS production by SH003 might induce ER stress. Thus, we next investigated whether SH003-induced ROS production causes ER stress. When we examined ER stress markers, NAC reduced SH003-induced eIF2α phosphorylation and CHOP expression (Figure 4C and D). Therefore, it is plausible that SH003 causes ER stress-mediated apoptosis *via* intracellular ROS production in breast cancer cells, subtype-independently.

CHOP is required for SH003-induced apoptosis. CHOP is a key player for ER stress-induced apoptosis (35, 36). SH003 increased CHOP protein expression levels (Figure 3A), which was blocked by 4-PBA (Figure 3B). As SH003 induces ER stress (Figure 3), we assumed that SH003 might increase *CHOP* gene expression. As expected, SH003 increased *CHOP* mRNA levels (Figure 5A), which is consistent with the SH003 increase of CHOP protein levels (Figure 3A). Therefore, we further examined whether SH003-induced apoptosis requires CHOP. When *CHOP* gene expression was silenced with *CHOP*

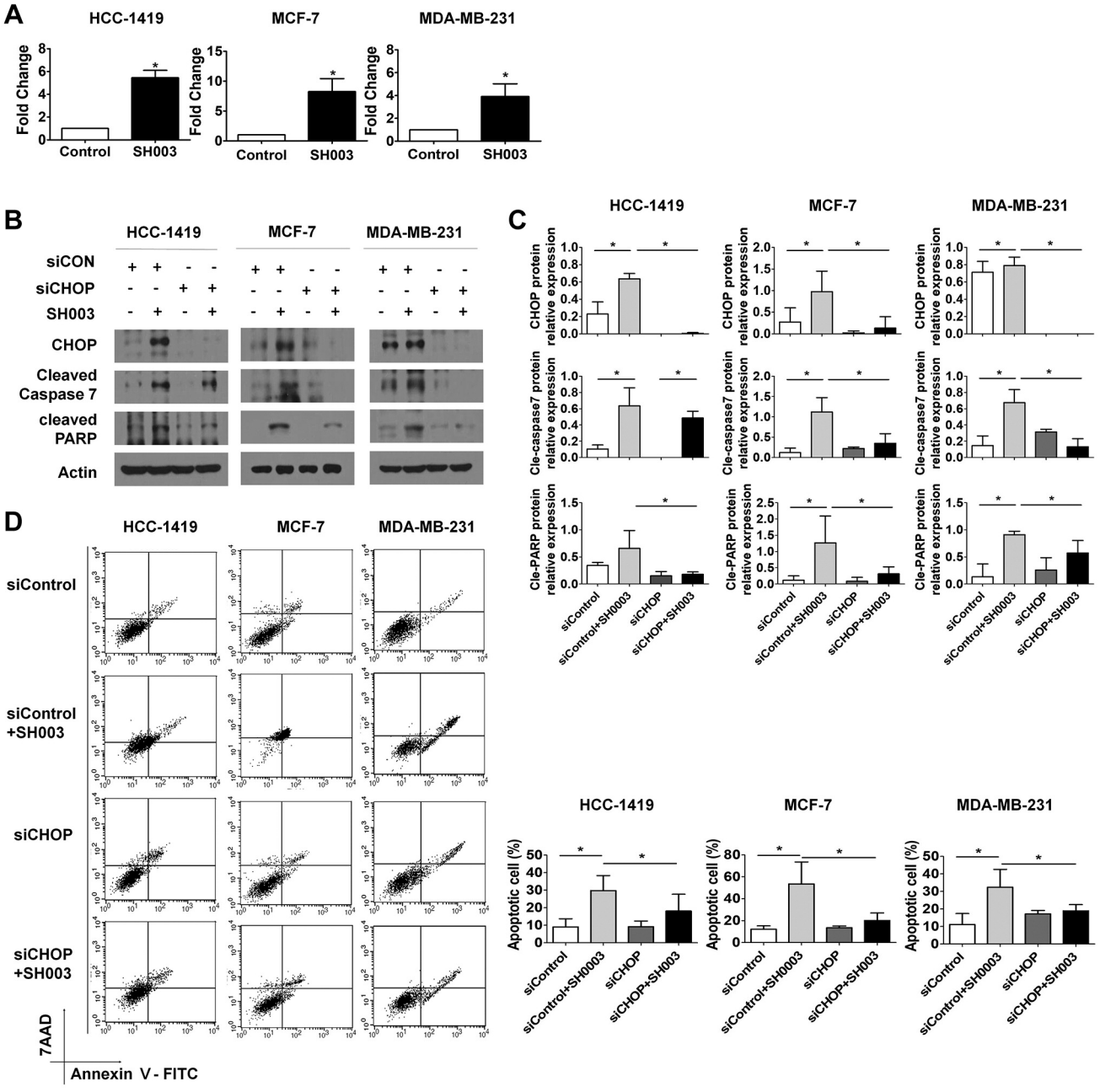

Figure 5. *SH003 requires CHOP for apoptosis of breast cancer cells. (A) SH003 induces CHOP mRNA expression. The cells were treated with SH003 at 500 μg/ml for 48 h and then CHOP mRNA levels were measured by quantitative real-time PCR. (B) CHOP gene silencing inhibits SH003-induced apoptosis. The cells transfected with either control siRNAs (siControl) or CHOP siRNAs (siCHOP) were treated with SH003 for 48 h, and then protein levels of CHOP, cleaved Caspase-7 and cleaved PARP were detected by western blot. (C) Relative protein levels of CHOP, cleaved Caspase-7 and cleaved PARP were measured. Bars indicate mean and standard deviation. (D) SH003-induced apoptosis requires CHOP. The cells transfected with either control siRNAs or CHOP siRNAs were treated with SH003 for 48 h, and then subjected to Annexin V-FITC and 7-AAD staining assays. Bar graphs shown as mean and standard deviation indicate apoptotic cell numbers. *p<0.05, one-way ANOVA followed by the Bonferroni post hoc test.*

siRNAs, *CHOP* gene silencing inhibited SH003-induced apoptosis (Figure 5B-D). *CHOP* knockdown also repressed SH003-mediated increase of cleaved PARP and cleaved Caspase-7 (Figure 5B and C). Accordingly, *CHOP* knockdown rescued SH003-induced apoptosis (Figure 5D). Therefore, SH003 requires CHOP to cause apoptosis of breast cancer cells.

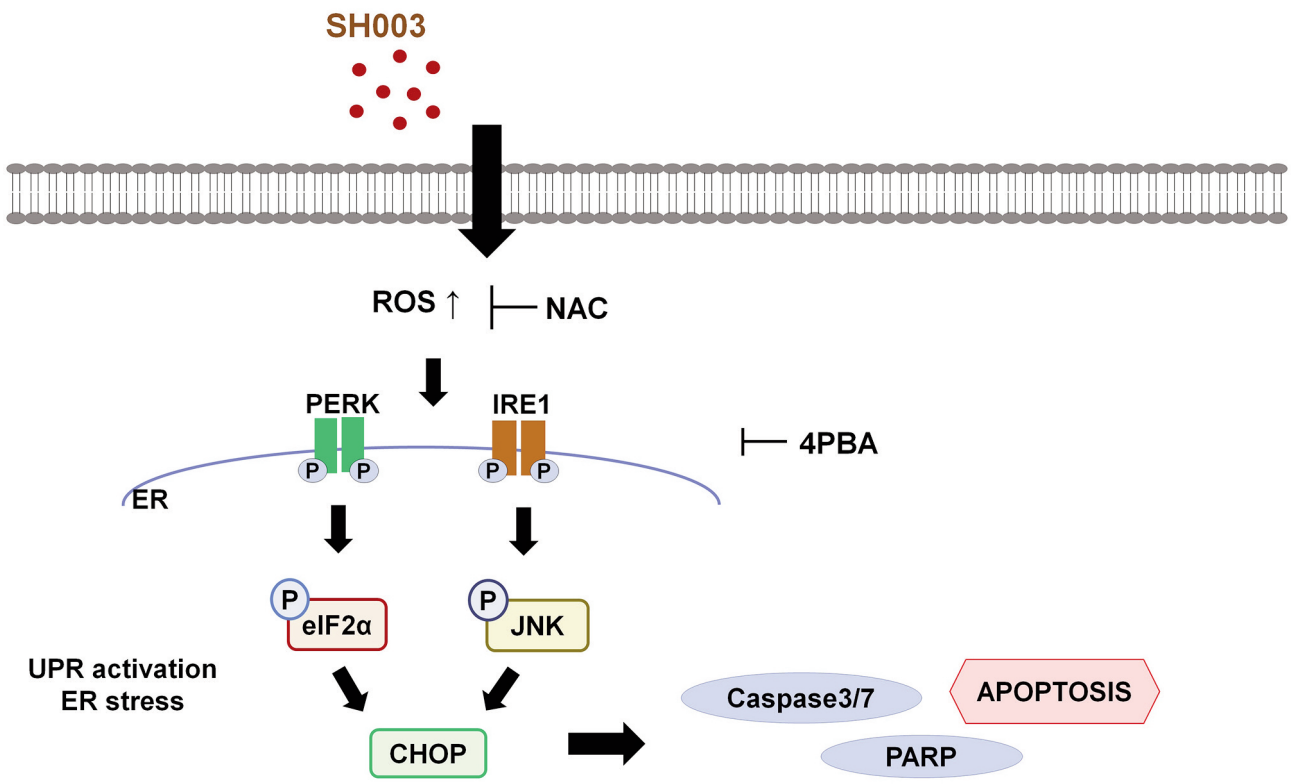

Figure 6. *Schematic image representing a mechanism of SH003-induced apoptosis of breast cancer cells. SH003 induces intracellular ROS production followed by ER stress, which results in apoptotic cell death independently of breast cancer subtype.*

Discussion

Herbal medicine named SH003 was originally developed for targeting highly metastatic triple-negative breast cancer cells based on the theory of the traditional Korean medicine (7). Our previous works revealed that SH003 causes apoptosis of triple-negative breast cancer cells (7, 8, 11). However, our first report showed that SH003 subtype-independently reduces a viability of breast cancer cells, although it mainly focused on triple-negative breast cancer cells (7). Moreover, our serial works revealed that SH003 causes apoptosis in various cancer cell types including breast, lung, gastric, prostate, and cervical cancer cells (7-15). However, we still need to clearly draw its mode of action in biochemical and cell biological views, although clinical studies for SH003 is ongoing and preclinical good laboratory practice toxicity tests have shown its safety (11, 18-20). Herein, we revealed that SH003 causes apoptosis of breast cancer cells through intracellular ROS production and ER stress in a breast cancer subtype-independent manner.

In our gene expression analysis, SH003 altered the expression pattern of 138 genes independently of the subtype of breast cancer cell lines. Interestingly, SH003 differentially altered the expression patterns of genes in different subtypes of breast cancer cells, although we statistically found common genes altered by SH003. This indicates that SH003 as a bundle of natural products targets multiple genes in breast cancer subtype-specific manner. Nevertheless, our previous and present data indicate that SH003 can be used to treat breast cancer independently of breast cancer subtypes and applied together with classical anti-cancer agents (7-9, 11, 15, 16). Therefore, understanding general modules for SH003 effect on cancer will improve our knowledge to convince SH003 effect in clinics.

Our gene expression data further showed that SH003 might alter genes involved in ER stress in a breast subtype-independent manner. ER stress is triggered by oxidative stress and *vice versa* (37). Our data showed that SH003 increases the level of ROS production independently of breast cancer subtype. Moreover, SH003 overcomes NAC inhibition of ROS generation, but 4-PBA rather increased SH003-triggered ROS production. In addition, NAC inhibited SH003-induced *CHOP* gene expression and eIF2α phosphorylation. Those data indicate that SH003-induced ROS production is located upstream of ER stress. Moreover, we found that *CHOP* gene silencing rescued SH003-induced apoptotic cell death. Thus, our data show that

SH003 causes apoptosis through the increased ROS production and ER stress in breast cancer cells (Figure 6).

Meanwhile, our previous studies show that SH003 inhibits EGFR phosphorylation in breast cancer and lung cancer cells and VEGFR phosphorylation in endothelial cells (7, 11, 14). Thus, SH003 is likely to inhibit the activation of receptor tyrosine kinases (RTKs). It has been known that RTKs activate ROS production and *vice versa* (38-40). Thus, we could image that SH003 may target RTKs, which is followed by the increase of intracellular ROS production and ER stress. Meanwhile, although SH003 is known to target STAT3 (7, 11, 16), it is unknown whether STAT3 is directly linked to ER stress in SH003-stimulated cancer cells. However, ER stress-related pathway inhibits STAT3-involved pathway and *vice versa* (41-44). ROS is also known to block STAT3 activation (45, 46). As the present study revealed that SH003 induces ROS production, it is plausible that SH003-induced ROS inhibits STAT3 activation and activates ER stress. Our ongoing study will reveal relations between ROS, STAT3 and ER stress in SH003-treated cancer cells.

We also need to consider multiple components in SH003. It is very plausible that each compound in SH003 may target various molecules within the cells. Although we still need more data to clearly understand the molecular functions of SH003, this study first answers how SH003 causes apoptosis of breast cancer cells independently of their subtype. This is important for understanding the SH003 function in the clinic, as breast cancer is highly heterogeneous (47-50). Our ongoing works will gather actions of all components in SH003 in the cells to draw a mode of action of SH003 holistically.

Conclusion

SH003 as herbal medicine was developed to treat cancer. Although its anti-cancer effects have been confirmed in various cancer cells, the underlying mechanisms are not yet clearly defined. This study shows that SH003 causes apoptotic cell death in various types of breast cancer cell lines by promoting intracellular ROS production and ER stress. Therefore, we suggest that SH003 may be a promising agent against breast cancer.

Conflicts of Interest

The Authors declare no competing interests.

Authors' Contributions

Lee SY designed the study, performed experiments and wrote the manuscript. Kim TH performed experiments. Ko SG, Choi WG and Chung YH worked on the design of the study together. Cheon C designed the study and managed the experiments. Cho SG designed the study, supervised the experiments, and wrote the manuscript. All Authors read and approved the final manuscript.

Acknowledgements

This work was supported by Korea National University of Transportation 2021, the National Research Foundation of Korea (NRF) grant funded by the Korea government (MSIT) (2017R1D1A1B03034996, 2020R1A5A2019413 and 2021R1F1A1057282) and the Ministry of Education (2021R1A6A1A03046418).

References

1 Sung H, Ferlay J, Siegel RL, Laversanne M, Soerjomataram I, Jemal A and Bray F: Global cancer statistics 2020: GLOBOCAN estimates of incidence and mortality worldwide for 36 cancers in 185 countries. CA Cancer J Clin *71(3)*: 209-249, 2021. PMID: 33538338. DOI: 10.3322/caac.21660

2 Yersal O and Barutca S: Biological subtypes of breast cancer: Prognostic and therapeutic implications. World J Clin Oncol *5(3)*: 412-424, 2014. PMID: 25114856. DOI: 10.5306/wjco.v5.i3.412

3 Dai X, Li T, Bai Z, Yang Y, Liu X, Zhan J and Shi B: Breast cancer intrinsic subtype classification, clinical use and future trends. Am J Cancer Res *5(10)*: 2929-2943, 2015. PMID: 26693050.

4 Kayl AE and Meyers CA: Side-effects of chemotherapy and quality of life in ovarian and breast cancer patients. Curr Opin Obstet Gynecol *18(1)*: 24-28, 2006. PMID: 16493256. DOI: 10.1097/01.gco.0000192996.20040.24

5 Hedigan K: Cancer: Herbal medicine reduces chemotherapy toxicity. Nat Rev Drug Discov *9(10)*: 765, 2010. PMID: 20885407. DOI: 10.1038/nrd3280

6 Ohnishi S and Takeda H: Herbal medicines for the treatment of cancer chemotherapy-induced side effects. Front Pharmacol *6*: 14, 2015. PMID: 25713534. DOI: 10.3389/fphar.2015.00014

7 Choi YK, Cho SG, Woo SM, Yun YJ, Park S, Shin YC and Ko SG: Herbal extract SH003 suppresses tumor growth and metastasis of MDA-MB-231 breast cancer cells by inhibiting STAT3-IL-6 signaling. Mediators Inflamm *2014*: 492173, 2014. PMID: 24976685. DOI: 10.1155/2014/492173

8 Choi EK, Kim SM, Hong SW, Moon JH, Shin JS, Kim JH, Hwang IY, Jung SA, Lee DH, Lee EY, Lee S, Kim H, Kim D, Kim YS, Choi YK, Kim HI, Choi HS, Cho SG, Kim JE, Kim KP, Hong YS, Lee WK, Lee JS, Kim TW, Ko SG and Jin DH: SH003 selectively induces p73 dependent apoptosis in triple negative breast cancer cells. Mol Med Rep 14(4): 3955-3960, 2016. PMID: 27599791. DOI: 10.3892/mmr.2016.5722

9 Woo SM, Kim AJ, Choi YK, Shin YC, Cho SG and Ko SG: Synergistic effect of SH003 and doxorubicin in triple-negative breast cancer. Phytother Res *30(11)*: 1817-1823, 2016. PMID: 27476488. DOI: 10.1002/ptr.5687

10 Choi YJ, Choi YK, Lee KM, Cho SG, Kang SY and Ko SG: SH003 induces apoptosis of DU145 prostate cancer cells by inhibiting ERK-involved pathway. BMC Complement Altern Med *16(1)*: 507, 2016. PMID: 27927199. DOI: 10.1186/s12906-016-1490-5

11 Choi YK, Cho SG, Choi YJ, Yun YJ, Lee KM, Lee K, Yoo HH, Shin YC and Ko SG: SH003 suppresses breast cancer growth by accumulating p62 in autolysosomes. Oncotarget *8(51)*: 88386-88400, 2016. PMID: 29179443. DOI: 10.18632/oncotarget.11393

12 Lee KM, Lee K, Choi YK, Choi YJ, Seo HS and Ko SG: SH003 induced G1 phase cell cycle arrest induces apoptosis in HeLa cervical cancer cells. Mol Med Rep *16(6)*: 8237-8244, 2017. PMID: 28944910. DOI: 10.3892/mmr.2017.7597

13 Kim TW, Cheon C and Ko SG: SH003 activates autophagic cell death by activating ATF4 and inhibiting G9a under hypoxia in gastric cancer cells. Cell Death Dis *11(8)*: 717, 2020. PMID: 32879309. DOI: 10.1038/s41419-020-02924-w

14 Jeong MS, Lee KW, Choi YJ, Kim YG, Hwang HH, Lee SY, Jung SE, Park SA, Lee JH, Joo YJ, Cho SG and Ko SG: Synergistic antitumor activity of SH003 and docetaxel *via* EGFR signaling inhibition in non-small cell lung cancer. Int J Mol Sci *22(16)*: 8405, 2021. PMID: 34445110. DOI: 10.3390/ijms22168405

15 Choi HS, Cho SG, Kim MK, Lee HJ, Moon SH, Jang HJ and Ko SG: SH003 enhances paclitaxel chemosensitivity in MCF-7/PAX breast cancer cells through inhibition of MDR1 activity. Mol Cell Biochem *426(1-2)*: 1-8, 2017. PMID: 27854072. DOI: 10.1007/s11010-016-2875-y

16 Seo HS, Ku JM, Lee HJ, Woo JK, Cheon C, Kim M, Jang BH, Shin YC and Ko SG: SH003 reverses drug resistance by blocking signal transducer and activator of transcription 3 (STAT3) signaling in breast cancer cells. Biosci Rep *37(6)*: BSR20170125, 2017. PMID: 28864784. DOI: 10.1042/BSR20170125

17 Choi HS, Kim MK, Lee K, Lee KM, Choi YK, Shin YC, Cho SG and Ko SG: SH003 represses tumor angiogenesis by blocking VEGF binding to VEGFR2. Oncotarget *7(22)*: 32969-32979, 2016. PMID: 27105528. DOI: 10.18632/oncotarget.8808

18 Cheon C, Kang S, Ko Y, Kim M, Jang BH, Shin YC and Ko SG: Single-arm, open-label, dose-escalation phase I study to evaluate the safety of a herbal medicine SH003 in patients with solid cancer: a study protocol. BMJ Open *8(8)*: e019502, 2018. PMID: 30082340. DOI: 10.1136/bmjopen-2017-019502

19 Cheon C and Ko SG: A phase I study to evaluate the safety of the herbal medicine SH003 in patients with solid cancer. Integr Cancer Ther *19*: 1534735420911442, 2020. PMID: 32186413. DOI: 10.1177/1534735420911442

20 Cheon C and Ko SG: Phase I study to evaluate the maximum tolerated dose of the combination of SH003 and docetaxel in patients with solid cancer: A study protocol. Medicine (Baltimore) *99(38)*: e22228, 2020. PMID: 32957363. DOI: 10.1097/MD.0000000000022228

21 Lee K, Ku JM, Choi YJ, Hwang HH, Jeong M, Kim YG, Kim MJ and Ko SG: Herbal prescription SH003 alleviates docetaxel-induced neuropathic pain in C57BL/6 mice. Evid Based Complement Alternat Med *2021*: 4120334, 2021. PMID: 34422067. DOI: 10.1155/2021/4120334

22 Han NR, Kim KC, Kim JS, Ko SG, Park HJ and Moon PD: The immune-enhancing effects of a mixture of Astragalus membranaceus (Fisch.) Bunge, Angelica gigas Nakai, and Trichosanthes Kirilowii (Maxim.) or its active constituent nodakenin. J Ethnopharmacol *285*: 114893, 2022. PMID: 34875347. DOI: 10.1016/j.jep.2021.114893

23 Bravo R, Parra V, Gatica D, Rodriguez AE, Torrealba N, Paredes F, Wang ZV, Zorzano A, Hill JA, Jaimovich E, Quest AF and Lavandero S: Endoplasmic reticulum and the unfolded protein response: dynamics and metabolic integration. Int Rev Cell Mol Biol *301*: 215-290, 2013. PMID: 23317820. DOI: 10.1016/B978-0-12-407704-1.00005-1

24 Hetz C: The unfolded protein response: controlling cell fate decisions under ER stress and beyond. Nat Rev Mol Cell Biol *13(2)*: 89-102, 2012. PMID: 22251901. DOI: 10.1038/nrm3270

25 Gardner BM, Pincus D, Gotthardt K, Gallagher CM and Walter P: Endoplasmic reticulum stress sensing in the unfolded protein response. Cold Spring Harb Perspect Biol *5(3)*: a013169, 2013. PMID: 23388626. DOI: 10.1101/cshperspect.a013169

26 Nishitoh H: CHOP is a multifunctional transcription factor in the ER stress response. J Biochem *151(3)*: 217-219, 2012. PMID: 22210905. DOI: 10.1093/jb/mvr143

27 Oyadomari S and Mori M: Roles of CHOP/GADD153 in endoplasmic reticulum stress. Cell Death Differ *11(4)*: 381-389, 2004. PMID: 14685163. DOI: 10.1038/sj.cdd.4401373

28 Chevet E, Hetz C and Samali A: Endoplasmic reticulum stress-activated cell reprogramming in oncogenesis. Cancer Discov *5(6)*: 586-597, 2015. PMID: 25977222. DOI: 10.1158/2159-8290.CD-14-1490

29 Yadav RK, Chae SW, Kim HR and Chae HJ: Endoplasmic reticulum stress and cancer. J Cancer Prev *19(2)*: 75-88, 2014. PMID: 25337575. DOI: 10.15430/JCP.2014.19.2.75

30 Walter P and Ron D: The unfolded protein response: from stress pathway to homeostatic regulation. Science *334(6059)*: 1081-1086, 2011. PMID: 22116877. DOI: 10.1126/science.1209038

31 Oakes SA: Endoplasmic reticulum stress signaling in cancer cells. Am J Pathol *190(5)*: 934-946, 2020. PMID: 32112719. DOI: 10.1016/j.ajpath.2020.01.010

32 Li Y, Guo Y, Tang J, Jiang J and Chen Z: New insights into the roles of CHOP-induced apoptosis in ER stress. Acta Biochim Biophys Sin (Shanghai) *47(2)*: 146-147, 2015. PMID: 25634437. DOI: 10.1093/abbs/gmu128

33 Zhang Z, Zhang L, Zhou L, Lei Y, Zhang Y and Huang C: Redox signaling and unfolded protein response coordinate cell fate decisions under ER stress. Redox Biol *25*: 101047, 2019. PMID: 30470534. DOI: 10.1016/j.redox.2018.11.005

34 Farooqi AA, Li KT, Fayyaz S, Chang YT, Ismail M, Liaw CC, Yuan SS, Tang JY and Chang HW: Anticancer drugs for the modulation of endoplasmic reticulum stress and oxidative stress. Tumour Biol *36(8)*: 5743-5752, 2015. PMID: 26188905. DOI: 10.1007/s13277-015-3797-0

35 Silva RM, Ries V, Oo TF, Yarygina O, Jackson-Lewis V, Ryu EJ, Lu PD, Marciniak SJ, Ron D, Przedborski S, Kholodilov N, Greene LA and Burke RE: CHOP/GADD153 is a mediator of apoptotic death in substantia nigra dopamine neurons in an *in vivo* neurotoxin model of parkinsonism. J Neurochem *95(4)*: 974-986, 2005. PMID: 16135078. DOI: 10.1111/j.1471-4159.2005.03428.x

36 Lei Y, Wang S, Ren B, Wang J, Chen J, Lu J, Zhan S, Fu Y, Huang L and Tan J: CHOP favors endoplasmic reticulum stress-induced apoptosis in hepatocellular carcinoma cells *via* inhibition of autophagy. PLoS One *12(8)*: e0183680, 2017. PMID: 28841673. DOI: 10.1371/journal.pone.0183680

37 Yoboue ED, Sitia R and Simmen T: Redox crosstalk at endoplasmic reticulum (ER) membrane contact sites (MCS) uses toxic waste to deliver messages. Cell Death Dis *9(3)*: 331, 2018. PMID: 29491367. DOI: 10.1038/s41419-017-0033-4

38 Wang TH, Chen CC, Huang KY, Shih YM and Chen CY: High levels of EGFR prevent sulforaphane-induced reactive oxygen species-mediated apoptosis in non-small-cell lung cancer cells. Phytomedicine *64*: 152926, 2019. PMID: 31454652. DOI: 10.1016/j.phymed.2019.152926

39 Paletta-Silva R, Rocco-Machado N and Meyer-Fernandes JR: NADPH oxidase biology and the regulation of tyrosine kinase receptor signaling and cancer drug cytotoxicity. Int J Mol Sci

14(2): 3683-3704, 2013. PMID: 23434665. DOI: 10.3390/ijms14023683

40 Chiarugi P and Cirri P: Redox regulation of protein tyrosine phosphatases during receptor tyrosine kinase signal transduction. Trends Biochem Sci *28(9)*: 509-514, 2003. PMID: 13678963. DOI: 10.1016/S0968-0004(03)00174-9

41 Meares GP, Liu Y, Rajbhandari R, Qin H, Nozell SE, Mobley JA, Corbett JA and Benveniste EN: PERK-dependent activation of JAK1 and STAT3 contributes to endoplasmic reticulum stress-induced inflammation. Mol Cell Biol *34(20)*: 3911-3925, 2014. PMID: 25113558. DOI: 10.1128/MCB.00980-14

42 Sanchez CL, Sims SG, Nowery JD and Meares GP: Endoplasmic reticulum stress differentially modulates the IL-6 family of cytokines in murine astrocytes and macrophages. Sci Rep *9(1)*: 14931, 2019. PMID: 31624329. DOI: 10.1038/s41598-019-51481-6

43 Banerjee K, Keasey MP, Razskazovskiy V, Visavadiya NP, Jia C and Hagg T: Reduced FAK-STAT3 signaling contributes to ER stress-induced mitochondrial dysfunction and death in endothelial cells. Cell Signal *36*: 154-162, 2017. PMID: 28495589. DOI: 10.1016/j.cellsig.2017.05.007

44 Kimura K, Yamada T, Matsumoto M, Kido Y, Hosooka T, Asahara S, Matsuda T, Ota T, Watanabe H, Sai Y, Miyamoto K, Kaneko S, Kasuga M and Inoue H: Endoplasmic reticulum stress inhibits STAT3-dependent suppression of hepatic gluconeogenesis *via* dephosphorylation and deacetylation. Diabetes *61(1)*: 61-73, 2012. PMID: 22124464. DOI: 10.2337/db10-1684

45 Chong SJF, Lai JXH, Eu JQ, Bellot GL and Pervaiz S: Reactive oxygen species and oncoprotein signaling-a dangerous liaison. Antioxid Redox Signal *29(16)*: 1553-1588, 2018. PMID: 29186971. DOI: 10.1089/ars.2017.7441

46 Linher-Melville K and Singh G: The complex roles of STAT3 and STAT5 in maintaining redox balance: Lessons from STAT-mediated xCT expression in cancer cells. Mol Cell Endocrinol *451*: 40-52, 2017. PMID: 28202313. DOI: 10.1016/j.mce.2017.02.014

47 Turner KM, Yeo SK, Holm TM, Shaughnessy E and Guan JL: Heterogeneity within molecular subtypes of breast cancer. Am J Physiol Cell Physiol *321(2)*: C343-C354, 2021. PMID: 34191627. DOI: 10.1152/ajpcell.00109.2021

48 Karthik GM, Rantalainen M, Stålhammar G, Lövrot J, Ullah I, Alkodsi A, Ma R, Wedlund L, Lindberg J, Frisell J, Bergh J and Hartman J: Intra-tumor heterogeneity in breast cancer has limited impact on transcriptomic-based molecular profiling. BMC Cancer *17(1)*: 802, 2017. PMID: 29187174. DOI: 10.1186/s12885-017-3815-2

49 Ellsworth RE, Blackburn HL, Shriver CD, Soon-Shiong P and Ellsworth DL: Molecular heterogeneity in breast cancer: State of the science and implications for patient care. Semin Cell Dev Biol *64*: 65-72, 2017. PMID: 27569190. DOI: 10.1016/j.semcdb.2016.08.025

50 Stingl J and Caldas C: Molecular heterogeneity of breast carcinomas and the cancer stem cell hypothesis. Nat Rev Cancer *7(10)*: 791-799, 2007. PMID: 17851544. DOI: 10.1038/nrc2212

Received July 4, 2022
Revised October 17, 2022
Accepted October 24, 2022